Blind Signal Identification

by

D. van der Geest

Blind Signal Identification

by

D. van der Geest

to obtain the degree of Master of Science
at the Delft University of Technology,
to be defended publicly on Tuesday February 15, 2018 at 10:00 AM.

Student number:	4110811	
Project duration:	March 20, 2017 – February 14, 2018	
Thesis committee:	Dr. ir. G. J. M. Janssen,	TU Delft, supervisor
	Dr. ir. R. Heusdens,	TU Delft
	Dr. ing. I. E. Lager,	TU Delft
	Ir. Vincent Voogt,	TNO

This thesis is confidential and cannot be made public until February 15, 2018.

An electronic version of this thesis is available at `http://repository.tudelft.nl/`.

TU Delft

Preface

This research project is the final work before receiving the masters degree in Electrical Engineering at the Delft University of Technology titled 'Blind Signal Identification'. For almost a year, work was done in the field of identification of wireless communication signals. This project was offered to me by TNO and is carried out under the supervision of both the TU Delft and TNO.

From a military point of view, there is a need to understand which signals are present in the increased congested and contested electromagnetic spectrum. The search for methods that can efficiently analyse all signals in this electromagnetic spectrum is a challenging task. Especially when there is no prior information available about a received signal, an extra level of difficulty is added. During this research project a framework is built in which those unknown signals can be analysed. The results are shown in this report.

D. van der Geest
Delft, February 2018

Contents

List of Figures

List of Tables

List of Symbols

A	Amplitude
B	Bandwidth
b	Bit sequence
C^{α}_{yyyy}	Cyclic temporal cumulant function
C_{42}	Fourth order cumulant with two conjugates
$CO^{\alpha}_{yy^*}$	Spectral Coherence Function
F_s	Sampling rate
f_c	Carrier frequency
f_{ch}	Frequency offset caused by the channel
f_{dop}	Doppler shift
f_o	Offset frequency
g	Pulse shaping filter
h	Multipath contributions
I	Information symbol
j	Discrete time index
k	Discrete time index
K	Upsample factor
l	Filter length
M	Modulation order
M_1	First order moment
N	Signal length
n	Discrete time index
P	Oversampling factor
r_{map}	Mapping function
r_{mod}	Modulation function
R^{α}_{yy}	Conjugate cyclic autocorrelation
$R^{\alpha}_{yy^*}$	Cyclic autocorrelation
s	Modulated signal
$S^{\alpha}_{yy^*}$	Spectral correlation function
T_s	Sample time
T_{sym}	Symbol time
v	uncorrelated noise
x	Original transmitted signal
y	Received signal
α	Cycle frequency
β	Roll-off factor

ϵ_A	Gain factor
λ	Threshold for energy detection
$\mathscr{H}$	Hypotheses
$\mathscr{L}$	Likelihood function
ϕ	Signal phase
Φ_{ch}	Phase offset caused by the channel
σ	Standard deviation
τ	Discrete time index
γ_{max}	Maximum value of the power spectral density

Abbreviations

ACG	Automatic Gain Control
ACI	Adjecent Channel Interference
ADC	Analog to Digital Converter
ASK	Amplitude Shift Keying
AMC	Automatic Modulation Classification
ALRT	Averaged Likelihood Ratio Test
AWGN	Additive White Gaussian Noise
BPSK	Binary Phase Shift Keying
CAF	Cyclic Autocorrelation function
CDP	Cyclic Domain Profile
CSP	Cyclostationary Signal Processing
CTCF	Cyclic Temporal Cumulant Function
CTMF	Cyclic Temporal Moment Function
DAC	Digital to Analog Converter
DFT	Discrete Fourier Transform
DSSS	Direct Sequence Spread Spectrum
DT	Decision Tree
GLRT	Generalized Likelihood Ratio Test
GMSK	Gaussian Minimum Shift Keying
FB	Feature Based
FFT	Fast Fourier Transform
FSK	Frequency Shift Keying
FHSS	Frequency-Hopping Spread Spectrum
HLRT	Hybrid Likelihood Ratio Test
HOCS	Higher Order Cyclostationary Statistics
HOS	Higher Order Statistics
ISI	Inter Symbol Interference
IQ	In-Phase Quadrature
LB	Likelihood Based
LOS	Lower Order Statistics
MSK	Minimum Shift Keying
OOK	On-Off Keying
OQPSK	Offset Quadrature Phase Shift Keying
PAM	Pulse Amplitude Modulation
PR	Pattern Recognition
PDF	Probability Density Function

QAM	Quadrature Amplitude Modulation
QPSK	Quadrature Phase Shift Keying
SCF	Spectral Correlation Function
SC	Spectral Coherence Function
SDR	Software Defined Radio
SNR	Signal to Noise Ratio
SOCS	Second Order Cyclostationary Statistics
WT	Wavelet Transform

1 Introduction

The Electronic Defense (ED) department of TNO is developing technologies to gain insight in the use of the radio spectrum. These technologies can be used in a military context. The correct detection and identification of signals in the radio spectrum can give valuable information about an opponent. According to [22], the intercepted radiated signals can be used for three purposes: identification of the unit transmitting, recovery of the transmitted message and the use of, and protection against, jammers. To identify signals from an unknown, and in general very large, pool of radio signals in the spectrum is a big challenge. For all these signals there is a need to identify the transmitter, the message it contains and where it's coming from. The focus of this research project will be to get this information from radio communication signals. A Software Defined Radio (SDR) is the basic platform that can be used to analyse the activities in the radio spectrum. SDR technology has the possibility to receive (tuning, sampling, detection and filtering) RF (Radio Frequency) signals. The digital samples can then be further processed by a processing device. Particularly for long time spectrum monitoring there is a need to efficiently process all data coming from the SDR in an automatic way.

The first step in identifying a communication signal is it's detection. In other words, the frequency bands where the wanted signal is present must be determined. Energy detection is the most common way to do so. Implementation is straightforward and prior knowledge of the signal is not needed [18] for this process. Another approach could be to use the cyclostationary properties of a signal for its detection. Detection becomes much more difficult when operating in a wideband and dense signal scenario. The use of, for example, FHSS (frequency-hopping spread spectrum) or DSSS (direct-sequence spread spectrum) schemes also gives rise to a challenge. The first of these radio transmission methods rapidly switches it's carrier among many different frequency channels whereas the latter results in a wideband channel with low SNR (signal to noise ratio). Another level of difficulty is added when different signals operate in the same frequency band. Those overlapping signals must be separated before they can be analysed. Ideally, the detection and separation will result in blocks of data that consist solely from one communication signal which has to be identified.

From a military point of view, a very important distinction between two types of signals must be made. First, there are communication signals of which the characteristics are known. Thus there is prior information available. For example, it is well known that GSM-900 operates in the 900 MHz band with a bandwidth of 200 KHz and a GMSK modulation scheme. For this type of signals one can correlate its properties with a database of known signals. In contrast, there are communication signals from which there is no prior information available. Its properties can't be correlated with known signals from a database. The focus of this research project will be to retrieve signal features for the identification of unknown communication signals i.e. Blind Signal Identification. Figure 1.1 shows a block diagram that differentiates between blind and non-blind signal identification. After successful detection and separation, complex valued IQ (in-phase, quadrature) data with a coarse estimate of some parameters can be obtained from the SDR device: bandwidth, carrier frequency, burst/continuous signal, SNR (signal to noise ratio) and power. The next step would be to check if these coarse parameters can be matched with known signals in a database. Coming back to the example of GSM, after detection and separation an oversampled signal with a rough estimate of its parameters will be left: carrier frequency of 900 MHz, bandwidth of 200 KHz, SNR, power and it's presence in the spectrum over time. These coarse parameters clearly match with the known GSM signal in the signal database. From an

opponent's point of view (in a military context), transmissions that have similar characteristics as known signals are less probable to be detected. Therefore, an extra check, exploiting the unique characteristics of GSM, could be done to identify it as a GSM signal. A brute force approach would be to tune a demodulator to this GSM channel and see if we end up with a signal that is expected. We could also make use of the unique burst structure to correctly identify it as a GSM signal. If after the extra check the signal is not the signal that was expected there will be 'no match' (Figure 1.1). Therefore the blind identification procedure will start.

On the other hand, if a signal is received from which those coarse parameters can't be matched, the blind identification procedure will be started as well. This means that, in a repeating loop, features from the unknown signal will be extracted and analysed. So from the received blocks of data, where we just have a coarse estimate of some parameters, we want to extract as much features as possible. The first step will be to look at the transmitter side of a communication system. So what kind of features does a communication signal have and how can we identify signals based on those features. One can think of modulation technique, bandwidth, symbol rate, single- or multi-carrier, pulse shaping etc. Another example could be the difference between continuous and burst signals. Determining the unique features of different communication signals will therefore be vital in blind signal identification.

Again referring to the feature extraction block from Figure 1.1, it is important to define which features are the most important ones in this military context. Generally speaking, if the modulation type, the (exact) carrier frequency and symbol rate are known, demodulation can be done. Therefore it was decided that those three parameters will be the most important ones. After demodulation the actual data that was sent by the transmitter can be analysed. Clearly, without any prior knowledge of the original signal it is still hard to find the actual message since it can be encrypted.

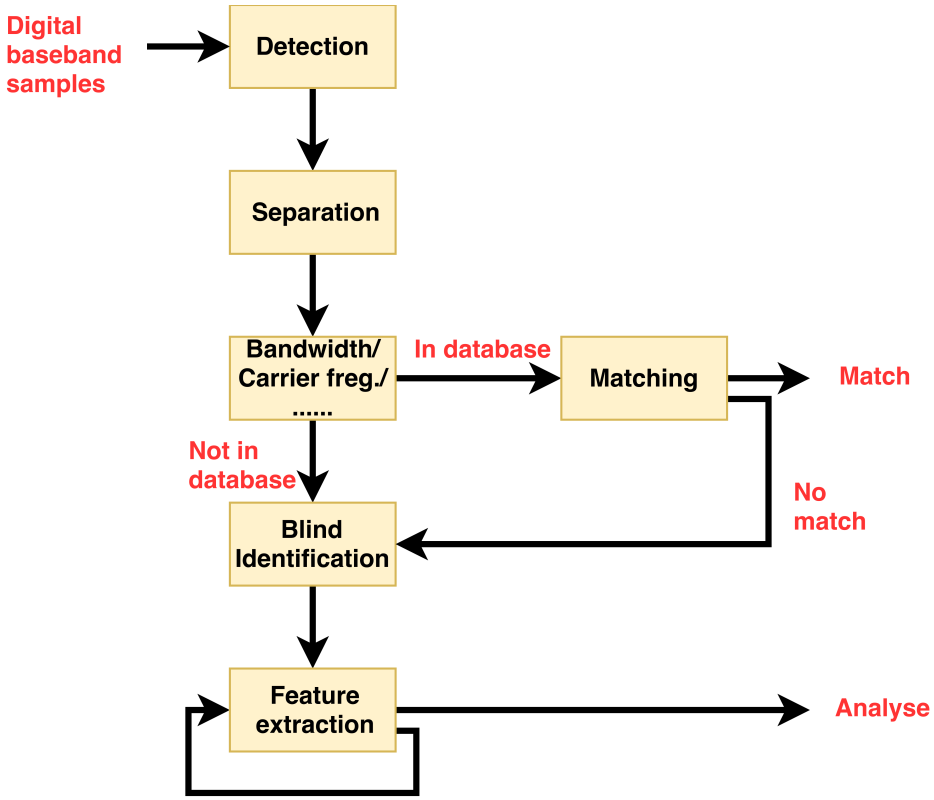

Figure 1.1: Block diagram when doing signal identification. A discrimination is made between 'blind' and 'non-blind' signal identification.

A block diagram related to automatic modulation classification (AMC) as shown in Figure 1.2 was proposed by [4]. It involves two steps before demodulation can be done: preprocessing and selection of the modulation classification algorithm. Preprocessing will include some or all of the following steps: detection, carrier frequency estimation, symbol period extraction, noise reduction, noise estimation etc. Depending on the

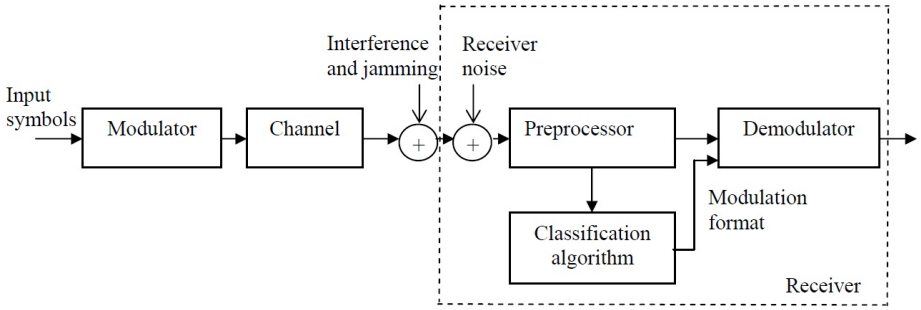

Figure 1.2: System block diagram proposed by [4] when performing automatic modulation classification. Unknown communication symbols are modulated and transmitted to a channel. This unknown signal will be contaminated with unknown signal contamination. At the receiver AMC will be performed as explained in this section.

classification algorithm chosen in the second step, the preprocessing can be done with different levels of accuracy. Some classification algorithms are more vulnerable to inaccurate estimates of unknown parameters like the carrier frequency. Furthermore, classification algorithms need different signal features with different levels of accuracy.

Again, it's very important to emphasize the difference between known (from a database) and unknown (coming from an unidentified transmitter) communication signals. From the previous discussion we arrive at the following problem statement:

Can we extract the symbol rate, carrier offset and modulation format from raw IQ-data when coarse estimates of the bandwidth, center frequency, SNR and burst length under signal contamination are available while also minimizing computational complexity?

To set some boundaries for the research, some assumption are made:

- The signal detection and separation will not be treated, we assume this has already been done. The received signal (by the SDR) therefore consists of blocks of IQ data, where we have exact knowledge of the sample rate. The signal is already mixed back to baseband, but can have a frequency offset. Some other coarse parameters are known: carrier frequency (already mixed down to baseband), SNR, power and bandwidth.
- Only digital modulated single carrier communication signals will be taken into account.
- The bandwidth and symbol rate of the received signal (mixed to baseband) will be (much) smaller than the sampling rate of the SDR. Generally, this is easily realizable with the hardware from nowadays when receiving a digital single carrier modulated signal. This implies that the full information content of the signal is captured within the data set (known as the Nyquist criteria).

This report consists of the following parts: Chapter 2 gives a signal model that was made related to the problem statement. Chapter 3 describes the statistical properties of a communication signal. Chapter 4 describes a study done on modulation classification when there is almost no prior information available about a received signal. Chapter 5 describes the preprocessing steps that must be performed before the actual modulation classification. It is a combination of a literature study and own work. In Chapter 6 a decision tree is built based on the work from the previous chapters. It also shows the identification results based on this decision tree. In Chapter 7 the work will be concluded and discussed. At last, in Chapter 8 some recommendations for future work will be given.

2

Signal Model

Communication is the process of transferring information from one place to another. In general, every communication system consist of three main components: transmitter, channel and receiver. This research will focus on the receiving part. However, it is important to have knowledge about the transmitter and channel and their implications on the received signal. These two parts of a communication link will influence the signal that is received by the SDR device. This chapter will describe a signal model for all those three parts. At first, an important distinction between two types of communication must be made: digital and analog. In digital communication, the transmitted signal is a waveform that can only take a discrete number of states. For example, a continuous time waveform alternating between two different frequencies can represent a logical '1' and '0'. As described in Chapter 1, we will only take digital single carrier modulated signals into account. Figure 2.1 illustrates a simplified version of a digital communication system having a transmitter, channel and receiver. A source wants to communicate with a sink using a channel. This source and sink can be, for example, people or computers. The channel can be a wireless link or a cable. First an input device is used to generate the data for communication which can be any type of sensor. The data reduction step will remove all irrelevant data. Source coding converts the input to a binary message. It can also be compressed depending on its application. For security measures the data can be encrypted. We use channel coding to add extra redundancy to the data during transmission. This is done by adding extra symbols to the information sequence in order to make it more robust against errors. At last, the symbols are modulated to create a waveform suited for transmission over the channel. After transmission through a certain channel, the receiver will do the inverse operations and in reverse order.

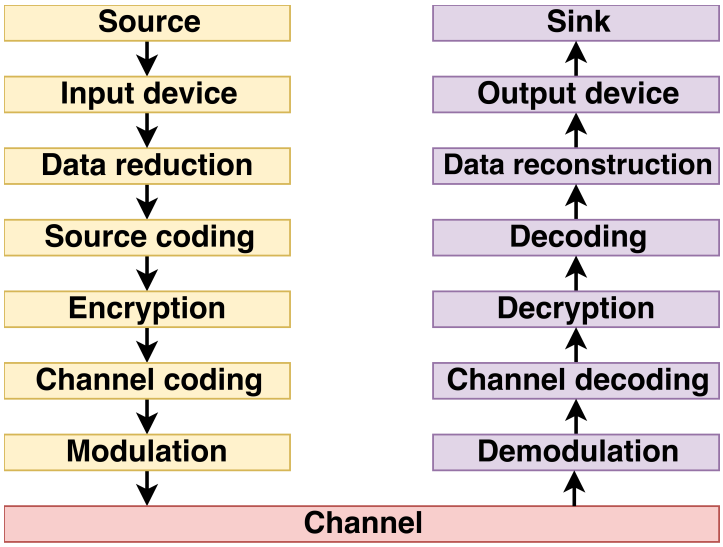

Figure 2.1: Communication system with a transmitter (yellow), channel and receiver (purple) adopted from [20].

In the case of blind signal identification there is no prior knowledge about the transmitter nor the channel.

This means that at the receiving device (SDR) the knowledge of the transmitting device and the channel can't be used to have a more educated guess of the transmitted signal. Therefore, Figure 2.1 can be simplified to Figure 2.2. This means that there is no knowledge about the yellow (transmitter) and red (channel part) from Figure 2.1. Figure 2.2 comes into play after the channel and before the demodulation part from Figure 2.1. The SDR device has flexible hardware, an analog front end, which mixes a communication signal to an IF (intermediate frequency). This signal will then be digitized by an analog to digital converter (ADC). The digital signal will then be down-mixed to baseband. The resulting baseband samples will then be processed. From these received baseband samples, one wants to find the original transmitted information. Taking the assumptions made in Chapter 1 into account, the received analog RF signal from Figure 2.2 is a single carrier digital modulated signal. The next sections will give a mathematical description of a transmitter, channel and receiver when doing blind signal identification adopted from [19]. Appendix A derives the equations from the next sections for a QPSK modulated signal. This will help the reader to have a better understanding of different modulation types.

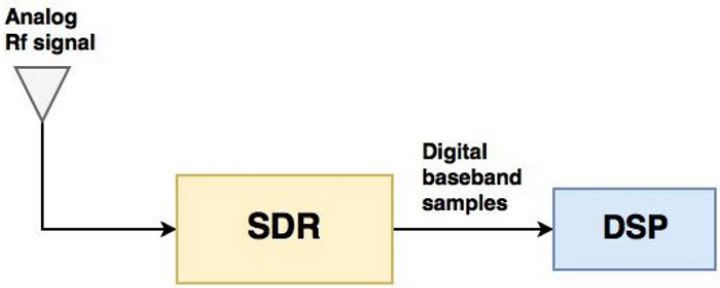

Figure 2.2: Simplified block diagram of a receiving SDR. An analog RF signal is transformed to digital baseband samples. This analog RF signal represents a digital single carrier modulated signal.

2.1. Transmitter

The description starts with an information source. This source generates a discrete representation of a signal. In this specific case this it would be a digital communication signal. When just two discrete states are possible, it is called an information bit. In other words, a communication signal is represented by a bit stream $b[j]$, where j is a discrete time index. This bit sequence can be mapped on a sequence of information symbols $I[k]$, where k is a discrete time index. For example, we can have 4 discrete states with information symbols $I[k] = [S_1, S_2, S_3, S_4]$ being equal to the bit sequence $b[j] = [00, 01, 10, 11]$. This mapping r_{map} from a bit sequence $b[j]$ to a sequence of information symbols $I[k]$ makes it possible to represent multiple bits with a single symbol. Those information symbols can be translated to waveforms through a process called modulation, represented by r_{mod}. All fundamental single carrier modulation techniques are built on varying one or more of the following properties of a waveform: phase, amplitude and frequency. The mapping from the information symbols $I[k]$ to the signal $s[k]$ is given in complex notation:

$$I[k] = r_{map}(b[j]) \tag{2.1}$$

$$s[k] = r_{mod}(I[k]) = A[k]e^{-i\phi[k]}, \tag{2.2}$$

The signal will be upsampled and filtered to change the spectral shape. The upsample factor is given by K. This means that $K-1$ zeros will be inserted after each information symbol. The upsampled signal will then passed trough a pulse shaping filter g with length l to remove high frequency images due to the upsample process. This pulse shaping filter will be further explained in Chapter 5. The main goal of this pulse shaping filter is to reduce the bandwidth before transmission.

$$z[n] = \begin{cases} s[k], & \text{for} \quad n = kK \\ 0, & \text{otherwise} \end{cases} \tag{2.3}$$

$$x[n] = (z * g)[n] = \sum_l z[l]\, g[n-l] \tag{2.4}$$

$$x[n] = \sum_l g[n-l]\, A(l) e^{-i\phi[l]} \tag{2.5}$$

where n is a discrete time index. Before transmission, the original baseband signal will be shifted to passband. The baseband signal will have spectral components between $[-f_b, f_b]$. After shifting the signal to passband with a carrier frequency f_c, the signal will have spectral components between $[f_c - f_b, f_c + f_b]$. Consequently the signal will keep the same bandwidth after this operation. This operation is shown by the first step in Figure 2.3.

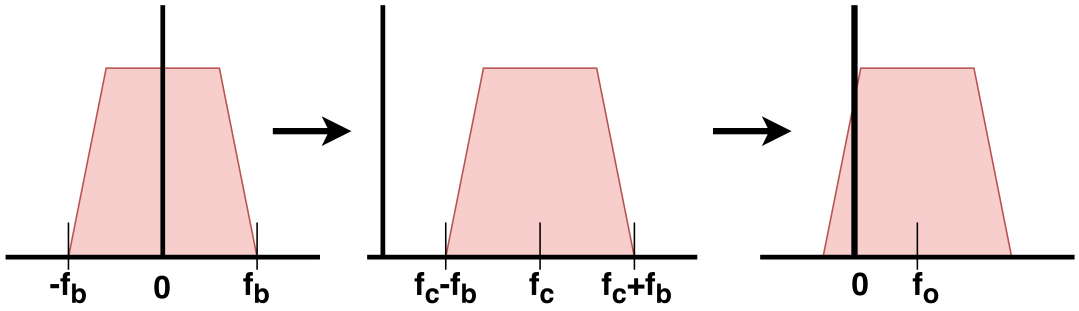

Figure 2.3: A signal with spectral components between $[-f_b, f_b]$ is shifted to passband with a carrier frequency f_c. After receiving and down-mixing the signal will have a carrier offset f_o.

The transmitted signal, in digital form, is now given by:

$$x[n] = \sum_l g[n-l]]\, A[l] e^{-i\phi[l]} * e^{-i2\pi f_c n T_s} \tag{2.6}$$

Where for every time index n there is a sum over the l filter taps and T_s is the sample time. So complex signal $A(n)e^{-i\phi(n)}$ is passed through a pulse shaping filter of length l. After that, the signal is shifted to passband by multiplying the filtered signal with the complex exponential $e^{-i2\pi f_c n T_s}$. This resulting digital signal is now translated to an analog continuous waveform by a digital to analog converter (DAC). This waveform can be described as:

$$x(t) = \sum_l g(t - l\,T_{sym})]\, A[l] e^{-i\phi[l]} * e^{-i2\pi f_c t} \tag{2.7}$$

where T_{sym} is the symbol period of the digital waveform. Clearly, only real world signals can be transmitted, so we take the real part of Equation 2.7. This waveform will be transmitted through the channel.

2.2. Channel

The channel is the medium in which the transmission symbols propagate to arrive at the receiver. Since there is no prior knowledge of any parameters of this channel it is simply modelled by Equation 2.8.

$$y(t) = \textbf{channel}(x(t)) \tag{2.8}$$

In the specific case of a wireless channel, which holds in a military context, a lot of theory has been developed on the modelling of this channel. It is well known that the medium between the transmitter and the receiver, known as the channel, can be characterized in three separate parts:

- Propagation path loss
- Shadowing and slow fading
- Multipath fading or fast fading

The received signal is also effected with a unknown noise component $v(t)$ which is uncorrelated with the original signal. Perfect knowledge of the channel would be ideal, since this information can be used in the case of blind signal identification. This can be done by equalization. Equalization is the process of compensating for the distortion caused by the channel. Non-blind channel estimation can be used when there is a feedback link between the transmitting device and the receiving platform. This means that you need access to the exact replica of the original transmitted signal to process the effect of the channel. Clearly, there is no access to this transmitted signal when doing blind signal identification so non-blind channel estimation is not possible. There is also a possibility of blind channel estimation which is called data-aided channel estimation. However, without any knowledge about the original signal, which can be any type of communication signal, it would be impossible to estimate and compensate for this channel. So the first step is to identify the limitations due to the channel. In a simplified form, the influence of the channel is modelled in the following way:

$$y(t) = \epsilon_A e^{-i\Phi_{ch}} * e^{-i2\pi f_{ch} t} \sum_s x(s) h(t - sT_{sym} - \tau) + v(t), \tag{2.9}$$

Where $x(s)$ is the symbol sequence, and $h(.)$ represents the multipath contributions. The unknown gain factor is given by ϵ_A and $|\epsilon_A| \leq 1$. The timing offset, τ, has the limitation/boundaries of $|\tau| \leq T_{sym}/2$. This assumption holds, because if $|\tau|$ becomes bigger then $T_{sym}/2$ it will result in a timing offset for the next symbol. The influence on the carrier frequency is modelled by f_{ch}. The Doppler shift f_{dop} is incorporated into this term. We assume that the the term f_{ch} is constant over the observation time. Furthermore, the phase offset is given by Φ_{ch} which is also constant over the observation time. The unknown noise term is given by $v(t)$ and is uncorrelated with the original signal $x(t)$. The thermal noise and any other uncorrelated noise is incorporated in this term. The effect of multipath is ignored. This assumption holds, since a narrowband model is used. Due to the model all multipath contributions sum to to a complex amplitude $\alpha e^{i\theta}$ which is incorporated in the terms ϵ_A and Φ_{ch}. Furthermore, the timing offset τ is removed, because the transmitted symbols are highly oversampled by the SDR. This will be further explained in the next section. This assumption results in a simplification of Equation 2.9:

$$y(t) = \epsilon_A e^{-i\Phi_{ch}} * e^{-i2\pi f_{ch} t} x(t) + v(t) \tag{2.10}$$

Now, by plugging in Equation 2.9 we will end up with:

$$y(t) = \epsilon_A e^{-j\Phi_{ch}} * e^{-i2\pi f_{ch} t} \sum_l g(t - lT_{sym}) A(l) e^{-i\phi(l)} * e^{-i2\pi f_c t} + v(t) \tag{2.11}$$

From the above assumptions it can be concluded that the channel will change the original transmitted waveform $x(t)$ in it's phase, amplitude and frequency as well as adding some unknown noise.

2.3. Receiver

The receiver picks up on the electromagnetic waves. The goal of a receiver in a communication system is to recover the original message as well as possible. However, when doing blind signal identification there is no knowledge about the original message. Therefore, the first goal is to extract as much information (features) from the received signal. First the received waveform will be mixed back to baseband. This is still done in the continuous time domain. An SDR has the ability to change its mixing frequency in order to analyse a wide frequency band. The maximum frequency range that can be recorded depends on the SDR. The resulting waveform, after it's mixed to baseband, is described by:

$$y(t) = \epsilon_A e^{-i\Phi_{ch}} * e^{-i2\pi f_o t} \sum_l g(t - lT_{sym}) A(l) e^{-i\phi(l)} + v(t) \tag{2.12}$$

This turns out to be the same equation as Equation 2.11 except for the term $f_c + f_{ch}$ which is combined to yield the frequency offset f_o. This means that mixing the signal back to baseband will never be perfect since some offset will always remain in the signal's frequency component. After down-mixing, the signal must be digitized by an analog to digital converter (ADC).

At the receiver side, the signal $y(t)$ is over-sampled by the SDR at rate P/T_{sym}. Here P is the oversampling factor and T_{sym} the symbol period of the original waveform. The generalized function of this oversampled waveform is::

$$y[n] = \epsilon_A e^{-i\Phi_{ch}} * e^{-i2\pi f_o n T_s} \sum_l g[n - l T_{sym}/T_s] A[l] e^{-i\phi[l]} + v[n] \tag{2.13}$$

The received waveform is oversampled by $P = F_s T_{sym}$ with F_s as the sampling rate of the SDR and $T_s = 1/F_s$. We can assume that the sampling rate of the receiver is much higher than the symbol rate and bandwidth of the original signal i.e. $T_s < T_{sym}$. This means that the Nyquist criteria is fulfilled. Therefore, we do not need prior information of the signal bandwidth. As a consequence of the oversampling by the SDR, the timing offset is not taken into account. This assumption holds, because if the signal is oversampled, an interpolation algorithm can be used to find the optimal sample point of each transmitted symbol. Hereby, it is assumed that the symbol rate is known. However, this is not the case when doing blind signal identification so this symbol rate must be determined before an interpolation algorithm can be used to find the optimal sample point.

From now on, Equation 2.13 will be the received signal model. Looking at the signal model gives a good overview of all the parameters that we have to deal with. We want to estimate the symbol period T_{sym}, carrier offset f_o and modulation type, while we have to deal with unknown parameters of the original signal as well as unknown signal contamination. The unknown parameter of the signal is the pulse shaping filter. The unknown channel parameters are the phase offset Φ_{ch}, amplitude attenuation ϵ_A and the complex noise term $v[n]$. So in conclusion: the SDR receives the waveform $y[n]$, consisting of the original waveform $x[n]$ plus unknown signal contamination.

3

Statistical and Cyclostationary Modelling

From the received signal $y[n]$, consisting of the original signal $x[n]$ plus unknown signal contamination, there is need to understand it's statistical properties. To do so, the theory of moments and cumulants will be adopted to describe the properties of a communication signal. Furthermore, the cyclostationary properties will be discussed since they exploit some unique characteristics of a communication signal. A distinction is made between Lower Order Statistics (LOS), Higher Order Statistics (HOS), Second Order Cyclostationary Statistics(SOCS) and Higher Order Cyclostationary Statistics (HOCS). It is important to notice that applying the LOS and HOS theory assumes that the statistical properties are constant over time whereas SOCS and HOCS do not make this assumption. This will be further explained in the next sections. For a worked out example, where the theory is applied on a QPSK signal, one can refer to Appendix A. This chapter will start with a very short summary of the stationary and cyclostionary statistics of a communication signal to make the reader familiar with the notations used. A received signal $y[n]$ can be described as second order cyclostationary in the following way:

$$R^{\alpha}_{yy^*}[n,\tau] = \sum_{n=0}^{N-1} y[n+\tau_1]\,y[n+\tau_2]\,e^{-i2\pi\alpha n T_s} \tag{3.1}$$

The term $R^{\alpha}_{yy^*}[n,\tau]$ represents the cyclic autocorrelation function (CAF). The subscript yy^* shows that we have a multiplication between the original signal $y[n]$ and a conjugated version of the original signal $y[n]^*$. The superscript α represents the cyclostationary behaviour (cycle frequency) of a signal as we see later in this chapter. Furthermore, T_s is the sample time and n a discrete time index. The lag vector is given by $\tau = [\tau_1, \tau_2]$. The CAF is thus a function of cycle frequency α, moment of observation n, lag vector $\tau = [\tau_1, \tau_2]$ and the number of (conjugated) multiplications as indicated by the subscript of R. The details follow in the next sections.

3.1. Lower Order Statistics

When a set of observed samples has the tendency to cluster around a particular value, this set can be characterized by it's statistical moments. The cumulant is also a statistical property of a probability distribution. Both statistics (cumulant and moment) can be defined as raw and centralized. Centralized moment means that we are calculating the moment about the mean whereas raw moment means we are calculating the moment about zero. The first order (raw) moment of the observed samples $y[n]$ of length N is defined as:

$$M_1[n] = E[y[n+\tau]] = E[y[n]] \tag{3.2}$$

A sample estimate is given by:

$$\hat{M}_1[n,\tau=0] = \frac{1}{N}\sum_{n=0}^{N-1} y[n+\tau] = \frac{1}{N}\sum_{n=0}^{N-1} y[n], \tag{3.3}$$

which is simply the sample mean. It can be seen that describing a signal in the LOS framework assumes that the delay vector τ equals zero and also the cycle frequency α equals zero. In other words, the statistics are assumed to be constant over time. Later in this chapter, the LOS will be related to SOCS. Therefore the same notations will be used for both LOS and SOCS. Equation 3.3 can be rewritten to yield:

$$\hat{M}_1[n] = \frac{1}{N}\sum_{n=0}^{N-1} y[n] = R_y^0[n, \tau = 0] \tag{3.4}$$

Since the information of the observed signal is present in either the phase, amplitude and frequency we can specifically look at one of those quantities. The observed complex signal $y[n] = A[n]e^{\phi[n]}$ (again of length N), has amplitude $A[n]$, phase $\phi[n]$ and frequency $f[n] = \big(\phi[n] - \phi[n-1]\big)\frac{1}{2\pi T_s}$ where T_s is the sample period. For example, the estimated first order moment of the amplitude is given by:

$$\hat{M}_{1_A}[n] = \frac{1}{N}\sum_{n=0}^{N-1} A[n] \tag{3.5}$$

The same procedure can be used to analyse the first order moment of the phase and frequency. If we want to analyse the moments for order higher than one, we have to take into account that we are working with complex numbers. Therefore, the second order moment can be different depending on the placement of the conjugations. The second order (raw) moment is defined as:

$$M_{20}[n] = E[y[n]y[n]] \tag{3.6}$$
$$M_{21}[n] = E[y[n]y^*[n]] \tag{3.7}$$

which again can be estimated from the sampled data:

$$\hat{M}_{20}[n] = \hat{M}_{22}[n] = R_{yy}^0[n] = \frac{1}{N}\sum_{n=0}^{N-1} y[n]y[n] \tag{3.8}$$
$$\hat{M}_{21}[n] = R_{yy^*}^0[n] = \frac{1}{N}\sum_{n=0}^{N-1} y[n]y^*[n] \tag{3.9}$$

The second order raw moment $\hat{M}_{20}[n]$ can already be used to discriminate between QPSK and BPSK. Figure 3.1 shows a scatterplot of $y[n]y[n]$ of a QPSK and a BPSK modulated signal (both with SNR=40dB). If we now take the average, one can see that for QPSK $\hat{M}_{20}[n] \approx 0$ and for BPSK $\hat{M}_{20}[n] \approx 1$. This is the easiest example of the use of lower order statistics. In section 3.2 an overview will be presented of some theoretical values of modulation types to show the discrimination capability of moments and cumulants.
The second order (raw) cumulant follows from the definition of the moment to cumulant function:

$$C_{20}[n] = M_{20}[n] - M_1^2[n] \tag{3.10}$$
$$C_{21}[n] = M_{21}[n] - M_1^2[n] \tag{3.11}$$

Also for the cumulant equations, the delay vector equals zero. The second order raw cumulant is equal to the second order centralized moment which is also known as the variance. The estimates of these quantities from sampled data follow from:

$$\hat{C}_{20}[n] = C_{yy}^0[n] = \hat{M}_{20}[n] - \hat{M}_1^2[n] \tag{3.12}$$
$$\hat{C}_{21}[n] = C_{yy^*}^0[n] = \hat{M}_{21}[n] - \hat{M}_1^2[n] \tag{3.13}$$

Note that the second order raw cumulant equals the second order raw moment when calculated for QPSK and BPSK, because the term $\hat{M}_1[n]$ (the mean value) equals zero. The definition of the cumulant function, with capital C, subscript yy^*, and superscript $\alpha = 0$ shows similarity with the function $R_{yy^*}^{\alpha}$ from the introduction

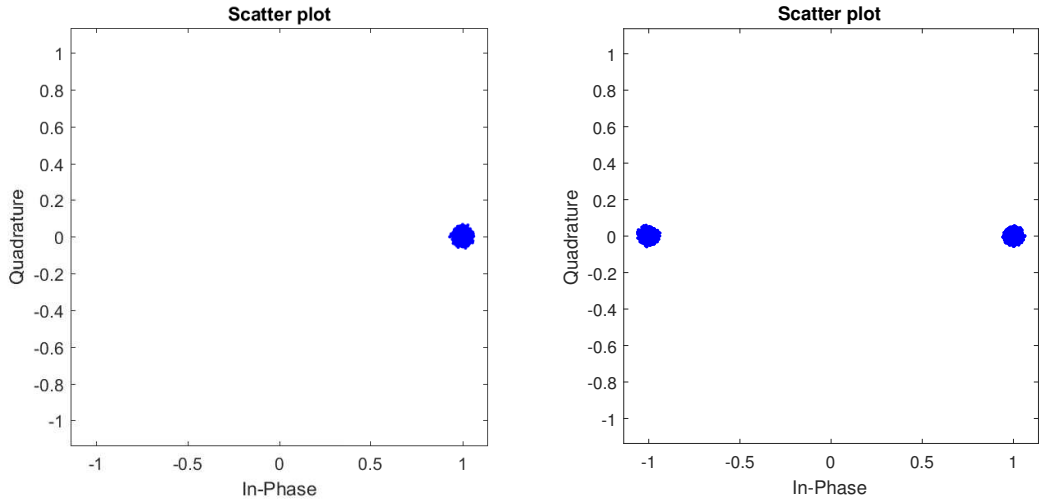

(a) BPSK modulated signal

(b) QPSK modulated signal

Figure 3.1: Illustrative example of the use of lower order statistics to discriminate between modulation types. Those scatterplots show the difference between the second order moment of both BPSK and QPSK for a SNR of 40dB.

of this chapter. This is done because now the theory of the stationary cumulant function can be expanded to the cyclostationary domain. The theory of second order moment and cumulant can also be slightly adapted to be a good discriminator. For example, according to [22] a useful statistical property of a communication signal is the standard deviation of the instantaneous phase:

$$\sigma_p = \sqrt{\frac{1}{N_s}\left(\sum_{A_n[n]>A_t} \phi^2[n]\right) - \left(\sum_{A_n[n]>A_t} \phi[n]\right)^2}, \tag{3.14}$$

where N_s is the number of samples that meet the criteria $A_n[n] > A_t$ with $A_n[n] = A[n]/(\frac{1}{N}\sum_{n=0}^{N-1} y[n])$. Only signal samples with an amplitude higher then a threshold A_t are taken into account. The threshold A_t is chosen to filter out low amplitude samples. This example can be related to the moment and cumulant equations. This can be concluded from the definition of the standard deviation, which is the square root of the variance. All previous equations form this section are time domain based statistics.

Another descriptive characteristic that is in de LOS framework are the transformation based statistics. Those statistics transform the time domain samples to the frequency domain. The maximum value of the power spectral density of the normalized and centred instantaneous amplitude can be used to discriminate between amplitude and non-amplitude modulations.

$$\gamma_{max} = \max|DFT(A_{cn})|^2/N, \tag{3.15}$$

$$\text{with} \quad A_{cn}[n] = A_n[n] - 1, \tag{3.16}$$

$$\text{where} \quad A_n = A[n]/\frac{1}{N}\sum_{n=1}^{N-1} a[n] \tag{3.17}$$

where $A_{cn}[n]$ is the centralized and normalized amplitude of the received sample set. It is centralized to remove the DC-component and normalized to prevent scaling problems in the final result. The Discrete Fourier Transform (DFT) is applied to show the amplitude fluctuations. The transformation to the frequency domain makes it a transformation based feature. In the chapters we will analyse the performance of these statistical properties in terms of modulation classification. Analysing signal in the LOS framework in the time domain as well as in the frequency domain result in low complexity calculations that can be used to discriminate between modulation types.

3.2. Higher Order Statistics

The use of higher order statistics as a statistical measure for complex valued signals is described in literature [17]. It was found out that higher order linear modulations such as QPSK and 8PSK have the same second order statistical moments and cumulants. Therefore, there is a need for statistical properties that uniquely define those higher modulation types. Again, we will have different moments and cumulants depending on the placement of the conjugations. The fourth order (raw) moment, with 2 conjugations is defined as:

$$M_{42}[n] = E[y[n]y[n]y^*[n]y^*[n]] \tag{3.18}$$

which can be estimated from sampled data as:

$$\hat{M}_{42}[n] = R^0_{yyy^*y^*}[n] = \frac{1}{N}\sum_{n=0}^{N-1} y[n]y[n]y^*[n]y^*[n] \tag{3.19}$$

Another descriptive statistic of a communication signal are its cumulants. If a communication signal has identical moments, the cumulants are identical as well. However, in some situations the cumulants are preferred. It is well known that the third and higher order cumulants of a normal distribution are equal to zero. If we relate this to modulation classification, a lot of (theoretical) problems try to find a certain modulation type in a white Gaussian noise channel. This noise has a normal distribution and therefore a cumulant value of zero. Another property that is described in literature is that if two random variables have independent statistics, the sum of it's cumulants equals the cumulant of their sum. Again coming back to the example of modulation classification, the (theoretical)cumulant value of QPSK in white Gaussian noise equals the cumulant value of a clean QPSK signal. The fourth order cumulant (with two conjugations) is defined as:

$$C_{42}[n] = \text{cumulant}\left(y[n]y[n]y^*[n]y^*[n]\right) \tag{3.20}$$

$$C_{42}[n] = E\big[y[n]y[n]y^*[n]y^*[n]\big] - E\big[y[n]y[n]\big]E\big[y^*[n]y^*[n]\big] - E\big[y[n]y^*[n]\big]E\big[y[n]y^*[n]\big] \tag{3.21}$$

The estimated $\hat{C}_{42}$ can be found from sampled data by replacing the expectation operator from Equation 3.20 for the sample average:

$$C_{42}[n] \approx \hat{C}_{42}[n] = C^0_{yyy^*y^*}[n] \tag{3.22}$$

Again, from this equation we can see that this method assumes that the statistical properties are constant over time since the value of τ equals zero. The resulting C_{42} at observation time n is assumed to be equal to the estimated C_{42} at time $n+\delta$, where δ is an arbitrarily chosen discrete time index. However, the statistical properties of a digital communication signal vary periodically with time. In the next sections, we will take this time dependency into account at the expense of more complexity. Table 3.1 shows the theoretical values of some cumulant values (up to order 6) of different modulation types. From this table it can be seen that a discrimination based on these theoretical cumulant values can be made. Only the cumulant equations up to order 4 are given, but this theory can be expanded to higher orders. However, calculating higher order moments or cumulant does not automatically mean that more modulation types can be classified. The crucial part in this approach is to have clear distribution of the IQ-points in a constellation plot. For example, a frequency offset will result in a (counter)clockwise rotation of these IQ-points resulting in wrong calculated moment values for a certain modulation type. In general, a received waveform, that is transmitted through a channel, will not have clear distribution of IQ-points. The channel results in distortion making it necessary to perform preprocessing (to remove the channel effects) or find methods that can deal with this distortion.

3.3. Second Order Cyclostationary Features

Many communication signals exhibit cyclostationary properties. When blindly analysing a signal there is clearly no knowledge about the signal features. No knowledge about the channel (noise, multipath, attenuation) makes it an even more difficult task. Cyclostationary signal processing has the potential of dealing with those conditions (noisy channels, frequency/timing offsets). For clarity reasons the theory will be treated

Table 3.1: Theoretical values of the stationary cumulants for three different modulation types.

Modulation	Order of Cumulant			
	4		6	
	Number of conjugations			
	0,4	2	1,5	3
BPSK	-2.0	-2.0	16.0	16.0
QPSK	1.0	-1.0	-4.0	4.0
8PSK	0.0	-1.0	0.0	4.0

both in the continuous time domain and discrete domain.

According to [16], signals that exhibit cyclostationary properties can be analysed by looking at 4 different parameters:

- Second-order temporal parameters
- Second-order spectral parameters
- Higher-order temporal parameters
- Higher-order spectral parameters

The second order parameters are a specific case of the more general higher order parameters. They will be treated separately, because they can be used for different purposes. We know that the autocorrelation function of a received complex signal is the correlation between the random variables of two time instants of the random signal:

$$R_{yy^*}(t_1, t_2) = E[y(t_1), y^*(t_2)] \tag{3.23}$$

Which can also be expressed in terms of the moment of observation t and lag τ. In the case of a wide sense stationary signal the value of the autocorrelation depends only on the lag parameter τ, and is therefore independent of the time of observation t.

$$R_{yy^*}(t_1, \tau) = R_{yy^*}(t_2, \tau) = R_{yy^*}(0, \tau) = R_{yy^*}(\tau), \tag{3.24}$$

which means that the autocorrelation function does not depend on the time instant t. Furthermore, by applying the Wiener-Khinchin theorem, the Fourier transform of the autocorrelation function (of a stationary signal) gives the power spectral density:

$$S_{yy^*}(f) = \int_{-\infty}^{\infty} R_{yy^*}(\tau) e^{-2\pi f \tau} d\tau \tag{3.25}$$

For signals that are not wide sense stationary, the autocorrelation does depend on the time instant. For the more specific case of cyclostationary signals, periodicity in the autocorrelation function with respect to the moment of observation t varies periodically in time as a result of the modulated data. The next equation describes the autocorrelation as a function of observation time t and lag parameter τ:

$$R_{yy^*}(t, \tau) = E[y(t + \tau/2) y^*(t - \tau/2)], \quad \text{where} \tag{3.26}$$

$$t_1 = t + \tau/2, \quad \text{and} \tag{3.27}$$

$$t_2 = t - \tau/2 \tag{3.28}$$

Information with respect to these time periodicities can be recovered using a Fourier decomposition of Equation 3.26

$$R_{yy^*}(t,\tau) = \sum_{\alpha} R^{\alpha}_{yy^*}(\tau) e^{i2\pi\alpha t}, \tag{3.29}$$

where $R^{\alpha}_{yy^*}$ is a Fourier series coefficient called the Cyclic Autocorrelation Function (CAF). The cycle frequencies α can be a useful property as we will see later. The CAF can be found by:

$$R^{\alpha}_{yy^*}(\tau) = \lim_{T\to\infty} \frac{1}{T} \int_{-T/2}^{T/2} R_{yy^*}(t,\tau) e^{-i2\pi\alpha t} dt \tag{3.30}$$

Rewriting Equation 3.30 for the discrete time domain gives:

$$R^{\alpha}_{yy^*}[\tau] = \lim_{N\to\infty} \frac{1}{N} \sum_{n=0}^{N-1} y[n+\tau_1] y^*[n+\tau_2] e^{-i2\pi\alpha n T_s} \tag{3.31}$$

This equation describes the CAF of a discrete time signal $y[n]$ as a function of the lag parameters τ and cyclic frequency α. Figure 3.2 shows the CAF for a stationary and a cyclostationary signal (BPSK modulated signal), where the lag vector is chosen as: $\tau = [0,\tau]$. The non-zero values for the CAF for different values of $\alpha \neq 0$ show that the BPSK-modulated signal is non-stationary. A general received complex waveform $y[n]$, consisting of the original waveform $x[n]$ plus unknown signal contamination, can be described as:

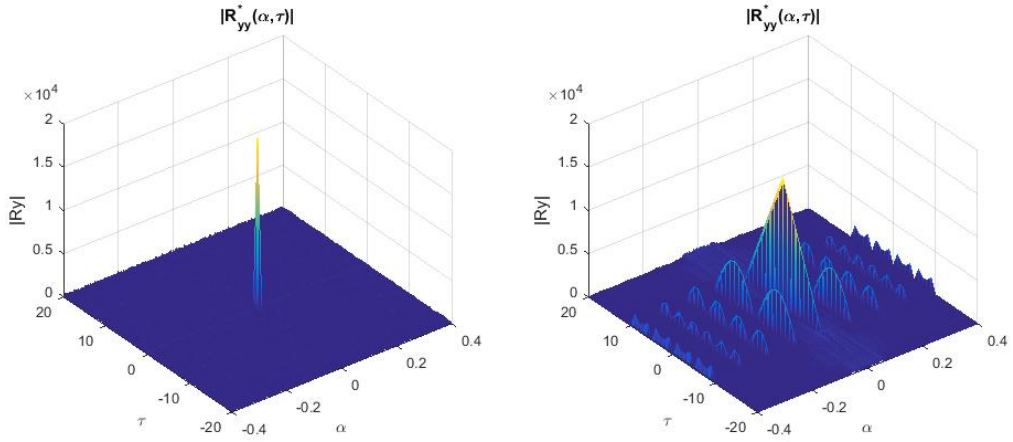

Figure 3.2: On the left the cyclic autocorrelation function of a stationary signal. On the right a cyclostationary signal. The symbol rate is $T_{sym} = 10T_s$

$$y[n] = A[n] e^{-i\phi[n]} \tag{3.32}$$

Applying the definition for the cyclic autocorrelation function to this received complex waveform function will result in:

$$R^{\alpha}_{yy^*}[n,\tau] = \sum_{n=0}^{N-1} y[n] y^*[n+\tau] e^{-i2\pi\alpha n T_s} \tag{3.33}$$

$$R^{\alpha}_{yy^*}[n,\tau] = \sum_{n=0}^{N-1} A[n] A[n+\tau] e^{-i(\phi[n]-\phi[n+\tau])} e^{-i2\pi\alpha n T_s} \tag{3.34}$$

$$\tag{3.35}$$

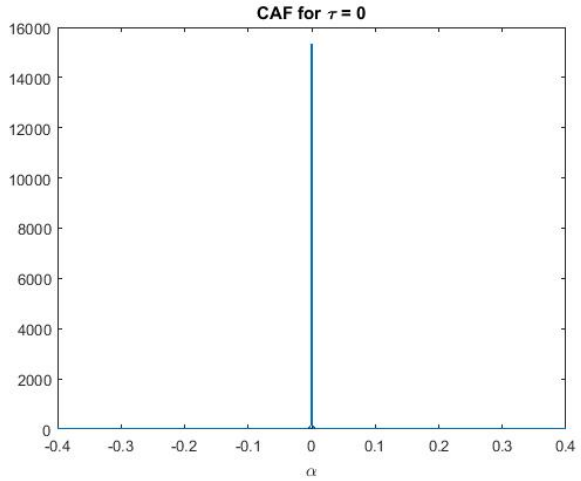

(a) CAF for the slice $\tau = 0$

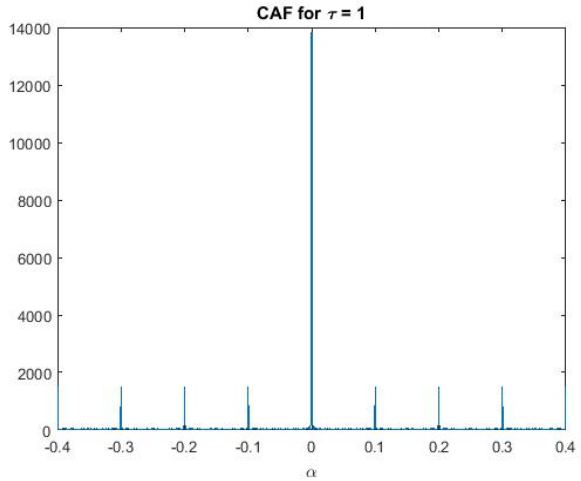

(b) CAF for the slice $\tau = 1$

Figure 3.3: The cyclic autocorrelation function $R^{\alpha}_{yy^*}[n,\tau]$ calculated for two different values of lag parameter τ. The symbol rate equals $T_{sym} = 10T_s$.

In Appendix A, it is mathematically shown how this digital CAF is resistant against frequency and phase offsets. The resulting plot for different values of α and τ for a BPSK modulated signal is given by Figure 3.2. If we take the value of lag parameter τ to be equal to 0, the CAF will not have periodicities as function of α as shown by Figure 3.3a. If the lag parameter is not equal to zero, this causes periodicities in the CAF. Figure 3.3b shows the CAF for a lag parameter τ equal to 1. This example shows that the choice of the lag value τ is the critical part in finding the actual cycle frequency α.

For some signals the conjugate autocorrelation function can have useful properties as well. It is defined as:

$$R_{yy}(t,\tau) = E[y(t+\tau/2)\,y(t-\tau/2)] \tag{3.36}$$

$$R_{yy}(t,\tau) = \sum_{\alpha} R^{\alpha}_{yy}(\tau)e^{i2\pi\alpha t} \tag{3.37}$$

Again, we will apply this definition to the same digital signal from Equation 3.32:

$$R^{\alpha}_{yy}[n,\tau] = \sum_{n=0}^{N-1} y[n]y[n+\tau]e^{-i2\pi\alpha nT_s} \tag{3.38}$$

$$R^{\alpha}_{yy}[n,\tau] = \sum_{n=0}^{N-1} A[n]A[n+\tau]e^{-i(\phi[n]+\phi[n+\tau])}e^{-i2\pi\alpha nT_s} \tag{3.39}$$

Both the conjugate and non-conjugate CAF and it's cycle frequencies α can be useful characteristics of unknown digitally modulated communication signals.

The theory of second order cyclostationarity can be further expanded by looking at its spectral correlation. Through an extension of the Wiener–Khinchin theorem [16] the spectral correlation function (SCF) is the Fourier transform of the CAF and defined as:

$$S^{\alpha}_{yy^*}(f) = \int_{-\infty}^{\infty} R^{\alpha}_{yy^*}(\tau)e^{-i2\pi f\tau}d\tau \tag{3.40}$$

So the cyclic autocorrelation function $R^{\alpha}_{yy^*}(\tau)$ is transformed to the frequency domain $S^{\alpha}_{yy^*}(f)$ with resolution $d\tau$. Similar to the CAF, also the conjugate version of the SCF has useful properties:

$$S^{\alpha}_{yy}(f) = \int_{-\infty}^{\infty} R^{\alpha}_{yy}(\tau)e^{-i2\pi f\tau}d\tau \tag{3.41}$$

A related function, the spectral coherence function (SC), is a normalized version of the SCF:

$$CO^{\alpha}_{yy^*}(f) = \frac{S^{\alpha}_{yy^*}(f)}{[S^{\alpha}_{yy^*}(f+\alpha/2)S^{\alpha}_{yy^*}(f-\alpha/2)]^{1/2}} \tag{3.42}$$

This normalization results in a value between 0 and 1 for $CO^{\alpha}_{yy^*}(f)$. Again we can apply those equations of the SCF to a received complex waveform as described by Equation 3.32. Rewriting Equation 3.40 for a sampled signal gives:

$$S^{\alpha}_{yy^*}(f) = \sum_{\tau=-\infty}^{\infty} R^{\alpha}_{yy^*}[\tau]e^{-i2\pi f\tau\Delta\tau} \tag{3.43}$$

$$S^{\alpha}_{yy^*}(f) = \sum_{\tau=-\infty}^{\infty}\sum_{n=0}^{N-1} y[n]y^*[n+\tau]e^{-i2\pi\alpha nT_s}e^{-i2\pi f\tau\Delta\tau} \tag{3.44}$$

$$S^{\alpha}_{yy^*}(f) = \sum_{\tau=-\infty}^{\infty}\sum_{n=0}^{N-1} A[n]A[n+\tau]e^{-i(\phi[n]-\phi[n+\tau])}e^{-i2\pi\alpha nT_s}e^{-i2\pi f\tau\Delta\tau} \tag{3.45}$$

So the same analogy of the continuous domain holds as for the discrete domain. The cyclic autocorrelation function of the received waveform $y[n]$ is calculated. After that it is transformed to the frequency domain by a DFT operation for every value of α.

3.4. Higher-Order Cyclostationary Features

The theory of Higher Order Cyclostationary Statistics (HOCS) is extensively studied in the literature. This section will highlight the most important theory. Coming back to the section about HOS, The nth-order/q-conjugate moment function is given by:

$$R^{0}_{y_q y_r^*}[n,\tau=0] = \frac{1}{N}\Big\{\prod_{i=1}^{q} y[n+\tau_i)]\prod_{j=1}^{r} y^{(*)}[n+\tau_j]\Big\}, \tag{3.46}$$

where we thus calculating the $(q+r)$th order moment with q non-conjugated and r conjugated version of the signal $y[n]$ are multiplied. The same theory as for SOCS can then be applied on this signal. This results in the following expression.:

$$R^{\alpha}_{y_q y_r^*}[\tau] = \lim_{N\to\infty} \frac{1}{N} \sum_{n=0}^{N-1} R_{y_q y_r^*}[n,\tau] e^{-i2\pi\alpha n T_s} \tag{3.47}$$

This term $R^{\alpha}_{y_q y_r^*}[\tau]$ is called the cyclic temporal moment function (CTMF). By applying the definition from Equation 3.20 we can also find the cyclic temporal cumulant function (CTCF), which is a combination of lower order cyclic moments. Determination of this complete CTCF is computationally expensive and visually hard to interpret. To decrease this complexity, we can search for specific cycle frequencies α in this CTCF. Furthermore, the function can also be evaluated for part of the vector $\tau = [\tau_1, ..., \tau_{r+q}]$ but also where some values in this τ-vector are kept constant. This method can be used for the classification of linear digital higher order modulation types. For example, the second order cyclostationary properties of QPSK and QAM16 are equal. If we then go to higher orders, those two modulation types have distinct cycle frequencies α [16].

This CTMF and CTCF can also be transformed to the frequency domain. However, this cyclic polyspectrum is difficult to compute and to interpret as the order increases. Furthermore, its usefulness in in the case of blind signal identification is not proven yet in literature. Therefore, there is no need to further discuss this theory.

3.5. Relation Between LOS and SOCS

Applying the theory of lower order statistics (LOS) implicitly implies that the received signal $y[n]$ is a stationary signal. So if we have a data set of length N, we assume that the statistical properties the set $y[1]....y[n]$ are equal to the statistical properties of the set $y[1+\tau]....y[n+\tau]$. In contrast, second order cyclostationarity assumes that is statistics vary periodically with time. In other words, the statistical properties the set $y[1]....y[n]$ are not only unequal to the statistical properties of the set $y[1+\tau]....y[n+\tau]$ but also vary periodically with time. See the next example, where we relate the time domain LOS to time domain SOCS:

$$\underbrace{R_{yy^*}[n,\mathbf{0}] = \frac{1}{N}\sum_{n=0}^{N-1} y[n]y^*[n]}_{\text{Stationary}} \Longleftrightarrow \underbrace{R^{\alpha}_{yy^*}[n,\tau] = \frac{1}{N}\sum_{n=0}^{N-1} y[n+\tau_1]y^*[n+\tau_2]e^{-i2\pi\alpha n T_s}}_{\text{Cyclostationary}} \tag{3.48}$$

So for the case of LOS we take the value of τ fixed to zero, whereas for SOCS the value of τ is not fixed. Another observation is that applying the moment or cumulant equations on a signal results in a 1 dimensional statistic (1 value). In contrast, SOCS results in a 3 dimensional statistic (Matrix) at the expense of more computations. I.e. the cyclic autocorrelation is a function of α and τ.

In the same way the spectral LOS can be related to spectral based SOCS:

$$\underbrace{S_{yy^*}(f) = \int_{-\infty}^{\infty} R_{yy^*}(\tau)e^{-2\pi f\tau}d\tau}_{\text{Stationary}} \Longleftrightarrow \underbrace{S^{\alpha}_{yy^*}(f) = \int_{-\infty}^{\infty} R^{\alpha}_{yy^*}(\tau)e^{-i2\pi f\tau}d\tau}_{\text{Cyclostationary}} \tag{3.49}$$

From this it's easy to see that for $\alpha = 0$, the spectral correlation function equals the normal power spectral density. So by calculating the SCF for $\alpha \neq 0$ we recognize the cyclostationary properties of the signal. Calculating the SCF can be done in a 'brute force' way which means that the SCF is calculated with resolution steps of $\Delta\alpha$. It was recognized, due to symmetry in this calculation, that it can be calculated more efficiently. This will be further explained in section 3.7. Figure 3.4 and Figure 3.5 graphically show the relation between time domain LOS and SOCS. Both figures show the CAF for a QPSK modulated signal where the red rectangle shows a subset of the complete CAF. The red rectangle in Figure 3.4 represents the CAF for a fixed value of $\alpha = 0.1$ and changing lag parameter τ. Therefore the CAF reduces to:

$$R^{0.1}_{yy^*}[n,\tau] = \sum_{n=0}^{N-1} y[n]y^*[n+\tau]e^{-i2\pi 0.1 n T_s} \tag{3.50}$$

Which is a time shifted version of the normal autocorrelation $R^{0}_{yy^*}[n,\tau] = \sum_{n=0}^{N-1} y[n]y^*[n+\tau]$. The red rectangle in Figure 3.5 shows the CAF for a fixed value of the lag parameter $\tau = 5$ and changing cycle frequency α. The CAF reduces to:

$$R^{\alpha}_{yy^*}[n,5] = \sum_{n=0}^{N-1} y[n]y^*[n+5]e^{-i2\pi\alpha nT_s} \tag{3.51}$$

Which can be seen as a DFT operation on the function $\sum_{n=0}^{N-1} y[n]y^*[n+5]$. Peaks appear at multiples of the symbol rate $T_{sym} = 10T_s$.

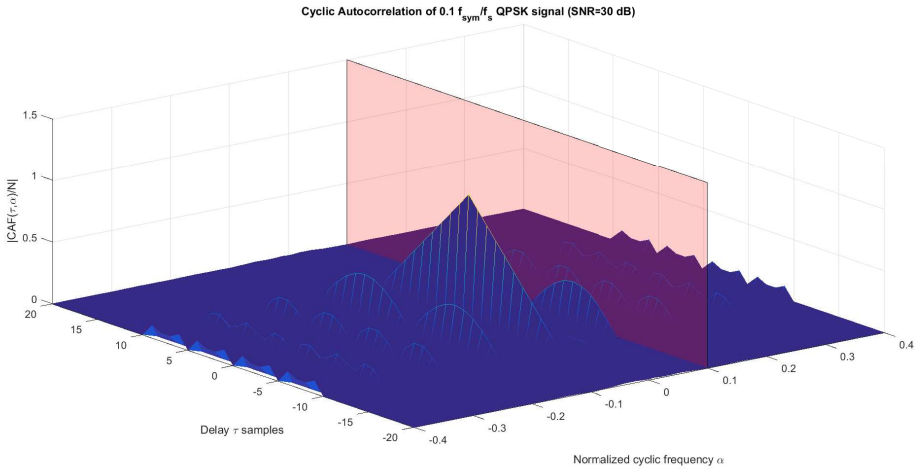

Figure 3.4: The red rectangle shows the CAF for a fixed value of $\alpha = 0.1$

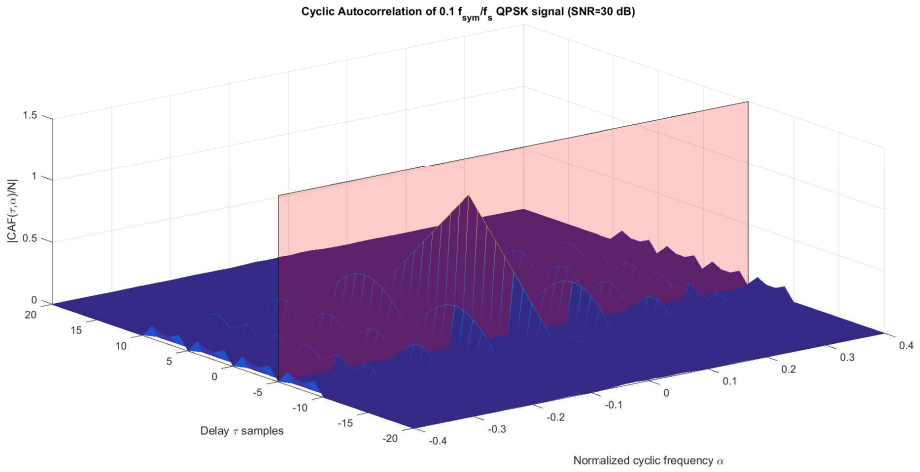

Figure 3.5: The red rectangle shows the CAF for a fixed value of lag paramter $\tau = 5$

3.6. Relation Between HOS and HOCS

Applying the theory from the previous section, we can find the relation between HOS and HOCS in the same way. The relation between the fourth order stationary moment (with 2 conjugates) and the fourth order CTMF (again with 2 conjugates) is given by:

$$\underbrace{R_{yyy^*y^*}[n,\mathbf{0}] = \frac{1}{N}\sum_{n=0}^{N-1} y[n]y[n]y^*[n]y^*[n]}_{\text{Stationary}} \Longleftrightarrow \underbrace{R^{\alpha}_{yyy^*y^*}[n,\tau] = \frac{1}{N}\sum_{n=0}^{N-1} y[n+\tau_1]y[n+\tau_2]y^*[n+\tau_3]y^*[n+\tau_4]e^{-i2\pi\alpha nT_s}}_{\text{Cyclostationary}} \tag{3.52}$$

The function $R_{yyy^*y^*}[n,\mathbf{0}]$ is evaluated for delay vector $\tau = [0,0,0,0]$ and $\alpha = 0$. On the other hand, the function $R^{\alpha}_{yyy^*y^*}[n,\tau]$ is evaluated for $\tau = [\tau_1,\tau_2,\tau_3,\tau_4]$ and chosen values of α. Clearly, the complexity for the complete statistical description in the HOCS framework is much higher. The details will be given in the next section.

3.7. Complexity Analysis

In order to compare the performance of the statistical descriptors, there is a need to look at their computational complexity. This is done by looking at the numbers of operations required. Again we start with signal $y[n]$ of N samples consisting of the original complex signal $x[n]$ plus unknown signal contamination. The complexity of calculating the LOS and HOS of this signal in time domain is of order N. For example the fourth order cumulant from Equation 3.20 needs only $4N$ complex multiplications. It can only be reduced by taking less samples. In practise, the N samples can be subdivided into smaller segments of length L. The statistical value of every segment is calculated and averaged over the number of segments. This will slightly increase the complexity.

If we look at transformation based LOS, the number of operations required increases. It is well known that calculating the DFT of a signal of length N requires $N\log(N)$ operations. The periodogram is then the squared magnitude of this DFT. We know that the periodogram is not a consistent estimate of the power spectral density of a random process. Therefore, there exist methods that average those periodograms to be a more consistent estimate of the real power spectral density. One of them is known as the Welch method. The Welch method divides the input signal $y[n]$ into L overlapping segments. The segments are convolved with the Welch window and the FFT is applied. Then the periodogram is computed of each window. The last step is to average the resulting periodograms to get the estimated power spectral density. The number of multiplications required, when we choose a 50 % overlapping window, is $\frac{N}{2}logN + N$ and the number of additions is NlogN. Depending on the scenario at hand we can change these parameters. So for example, if we need a high resolution power spectral density of a signal to compare it with a known template (i.e non blind signal identification) more computations are required. On the other hand, if the power spectral density is used as a coarse estimate for the bandwidth, a lower resolution can be chosen requiring less computations.

The complexity of time domain SOCS (Cyclic Autocorrelation Function) depends on the chosen resolution in cycle frequency $\Delta\alpha$. Also the number of calculated lags τ and the signal length N are parameters that influence complexity.

The complexity of frequency domain SOCS (Spectral correlation function) at first depends on the chosen cycle frequency $\Delta\alpha$. The same theory, in relation to the number of operations, holds as for spectral based LOS. Spectral LOS calculates the SOCS for the value of $\alpha = 0$ whereas de spectral based SOCS is calculated for a multiple values of $\Delta\alpha$. So the number of operations increases when the number of calculated values α increases.

In order to characterize a signal as a time domain HOCS a lot of operations are required. As the order M grows, the number of lags $\tau = [\tau_1,..,\tau_m]$ for which the cyclic temporal cumulant function must be evaluated increases exponentially. In the next subsection, it will be explained why not the complete set of lags has to be calculated but only a subset of this delay vector.

Table 3.2 gives a short overview of all he discussed statistical methods. It gives an order of magnitude estimation of the computational complexity.

3.7.1. Reducing Complexity

From this table it's clear that the complete characterization of a communication signal as a (higher order) cyclostationary signal, requires a lot of computations. This complexity can be reduced by looking for specific information in the cyclostationary feature space. Recall the equation for the digital CAF:

$$R^{\alpha}_{yy^*}[n,\tau] = \sum_{n=0}^{N-1} y[n+\tau_1]\,y^*[n+\tau_2]\,e^{-i2\pi\alpha nT_s} \tag{3.53}$$

	Number of multiplications	Number of additions	Comments
LOS (time domain)	N	N	The complexity is of order N. Depending on the exact statistic (mean, variance) the complexity can be different
LOS (spectral)	N*log(N)		The complexity of this operation requires at least NlogN operations, but can increase depending on the number of (non-)overlapping windows
HOS	M*N	M*N	If the order increases M, the complexity increases linearly.
SOCS (time domain)	$\alpha * N * \tau$		
SOCS (spectral)	N*log(N)*α		
HOCS	α*N*τ^{M-1}		If the order increases the possible delay vectors (and thus number of operations) increase exponentially.

Table 3.2: Complexity of the different statistical descriptions of a communication signal

This function can for example be evaluated for a limited amount of lags τ to find the symbol rate. In general, especially in a blind signal scenario where there is no prior knowledge about the carrier frequency, symbol rate, modulation type and transmit filter, it is hard to predict for which exact lag parameter τ the CAF must be evaluated to find the symbol rate. By first recognizing the symmetry in this calculation the number of computations can be reduced. By also recognizing that the strongest peaks at cycle frequency $\alpha = T_{sym}$ appear around $\tau = 0$ (but not necessarily at exact 0) the number of computations can be further reduced. This will be further explained in chapter 6.

Some linear digital modulations have the same second order cyclostationary properties. A well known example is QPSK and QAM16. Those signals can be separated by looking at it's HOCS features. But instead of evaluating this function for all possible lags τ and all values of α the complexity dramatically decrease if we evaluate this equation only for a smart choice of those parameters. First the second order cycle frequencies α are calculated. After that the CTCF is then evaluated only for these specific cycle frequencies and a smart choice of the lag vector τ. An example of a lag vector is $\tau = [\tau_1, 0, 0, 0]$ where τ_1 is chosen in way that the symmetry in this calculation is recognized as well as that the highest peaks for the cycle frequency α appear around $\tau = 0$.

4

Automatic Modulation Classification

4.1. Introduction

Automatic modulation classification (AMC) can be described as the stage between signal detection and demodulation. It has been part of research for more then twenty-five years and it's widely used in military and civilian applications. AMC can be roughly divided into two broad sub-methods: likelihood-based (LB) and feature based (FB). Generally, the likelihood-based methods can be seen as a multiple-hypothesis testing problem, where the received waveform is compared with a set of known modulation types. Feature based methods use signal characteristics to classify modulation schemes.

4.2. Likelihood Based

The probability density function (PDF) of the incoming waveform conditioned on the embedded waveform gives the information needed for classification [14]. This definition is the general description for all likelihood-based classifiers. In other words, for this method the probability density function of the received signal is compared with a predefined set of known modulation types. If we want to calculate the likelihood function of a received signal $y[n]$ in a channel and only AWGN (additive white Gaussian noise) with known variance σ, then the likelihood function $\mathscr{L}$ is given by [22]:

$$\mathscr{L}(y[n]|M,\sigma) = p(y[n])|M,\sigma), \tag{4.1}$$

Where M is the number of modulation types from a predefined set. The likelihood function $\mathscr{L}$ is the probability that the received waveform is from modulation type M. This can be seen as a maximum likelihood classifier, where except for the modulation type, all parameters are determined or known. Rewriting this equation by adding the definition of the PDF of the received signal in a AWGN channel one gets:

$$\mathscr{L}(y[n]|M,\sigma) = \sum_{m=1}^{M} \frac{1}{M} \frac{1}{2\pi\sigma^2} e^{-\frac{|y[n]-A_m|^2}{2\sigma^2}}, \tag{4.2}$$

Where A_m is the modulation symbol that belongs to modulation type M. The likelihood of every modulation type from the set is calculated through the likelihood value between all symbols A_m from modulation type M and the observed sample $y[n]$. This can be done for the complete observed sample set $\mathbf{y}$. The maximum likelihood for the complete sample set is found by multiplying the likelihoods of each sample:

$$\mathscr{L}(\mathbf{y}|M,\sigma) = \prod_{n=1}^{N} \sum_{m=1}^{M} \frac{1}{M} \frac{1}{2\pi\sigma^2} e^{-\frac{|y[n]-A_m|^2}{2\sigma^2}}, \tag{4.3}$$

From this equation it is clear that we need perfect knowledge of the channel. Unknown parameters such as frequency offset, phase offset and multipath loss are the limiting factors in a maximum likelihood based classifier. There are three general methods that can deal with unknowns which are: ALRT (averaged likelihood

ratio test), GLRT (generelized likelihood ratio test) and HLRT (hybrid likelihood ratio test) and are well described in [21]. The ALRT will be shortly discussed to show its working principle. In this ALRT all unknown parameters are replaced with the integral of the probabilities of their possible values. So we need to determine the distribution of all (unknown) parameters. For example, if a modulated signal in a AWGN channel where only the (constant) phase offset is unknown we need to find their possible phase offsets and their probabilities. This likelihood can be described as[22]:

$$\mathscr{L}_{ALRT} = \int_{\theta_0} \mathscr{L}(\mathbf{y}|\theta_0) f(\theta_0|\mathscr{H}) d\theta = \int_{\theta_0} \prod_{n=1}^{N} \sum_{m=1}^{M} \frac{1}{M} \frac{1}{2\pi\sigma^2} e^{-\frac{|y[n]-\alpha e^{-j\theta_0} A_m|^2}{2\sigma^2}} f(\theta_0|\mathscr{H}), \tag{4.4}$$

Where $\mathscr{L}(\mathbf{y}|\theta_0)$ is the likelihood with a given phase offset θ_0 and $f(\theta_0|\mathscr{H})$ is the probability of constant phase offset θ_0 under the hypothesis $\mathscr{H}$. Hypothesis $\mathscr{H}$ means that the signal $y[n]$ is from modulation type M. When only the constant phase offset is unknown, its already a complex operation. In a blind scenario, there are a lot more unknowns and these can also change over time. Therefore, one needs quite a lot of preprocessing to estimate the probability distribution of all unknown parameters of the received signal taking all channel conditions into account. Although likelihood methods turn out to have the best performance in terms of correct classification when the channel conditions and signal characteristics are known, it's complex to implement when this information is not available. It is also known to have high computational complexity since the likelihood function needs to be determined for all unknown variables for each known modulation type. This also means that we are limited to a predefined set of modulation types. So this methods can't deal with unknowns.

4.3. Feature Based

Feature based (FB) methods for AMC is the most commonly used technique when finding the modulation type without prior information of the original signal. Generally, FB methods can perform close to LB methods but have lower computational complexity. In [7] an overview is provided of FB methods for AMC and a separation is made between 3 different types of AMC features: instantaneous time domain features, transformation based features and statistical features. This subsection will follow the same categorization. Those 3 categories can than be subdivided into smaller categories. When the needed features are extracted the actual modulation classification can be performed. Some examples of AMC features will be given in the next sections.

4.3.1. Feature Extraction

In [22], some commonly used time domain features to distinguish between different modulation types are summarized. For example, the variance in the absolute, instantaneous phase can be used to classify phase and non-phase modulated signals.

$$\sigma_p = \sqrt{\frac{1}{N_C}\left(\sum_{A_n[n]>A_t} \phi^2[n]\right) - \left(\sum_{A_n[n]>A_t} \phi[n]\right)^2}, \tag{4.5}$$

Where the variance of the phase ϕ is calculated for the received samples where the amplitude $A_n[n]$ is higher then a certain threshold A_t. The sample size that has higher amplitude than the threshold is of length N_c. Generally, instantaneous time domain features have the drawback of being vulnerable to timing, frequency and any other type of signal contamination. If a received non-phase modulated signal (ASK,OOK) has some frequency offset it will be misclassified if it is analysed by Equation 4.5. This can directly be concluded from the fact that a frequency offset will change the phase of the received signal. This is a relevant problem when doing blind modulation classification. Thus there is need for preprocessing to remove the signal contamination that reduces the classification performance. Some time domain features are less vulnerable (without preprocessing) to signal contamination, making it a candidate for blind signal identification without preprocessing.

The second category is based on transformation from the time domain to some other domain in order to extract features from the unknown signal. Both the Fourier transform and the Wavelet transform are candidates

that are studied in the literature. For example, the maximum value of the power spectral density of the normalized and centred instantaneous amplitude can be used to discriminate between constant envelope and non-constant envelope modulations [22]:

$$\gamma_{max} = \max|\mathrm{DFT}(A_{cn})|^2/N, \quad \text{with} \tag{4.6}$$

$$A_{cn}[n] = A_n[n] - 1 \quad \text{and} \tag{4.7}$$

$$A_n = A[n]/\frac{1}{N}\sum_{n=1}^{N-1} a[n] \tag{4.8}$$

Where A_{cn} is the centred and normalized version of the amplitude $A[n]$ of the received waveform. This method can deal with frequency and phase offsets as well as noisy channels. A threshold for γ_{max} must be determined based on theory or training data to make the actual distinction. In Chapter 6, this method will be further explained because it turned out to have good performance even for a highly contaminated signal. Another transformation based feature is the Wavelet Transform (WT). Features from the WT contain time domain as well as frequency domain information. This method has the advantage of its ability to deal with noisy channels [6]. However only a few different (linear) modulation types can be classified with this method. Therefore the Wavelet Transform based features are not further studied.

The third subgroup is based on the statistical features of the unknown signal. One commonly used feature for AMC of a single carrier modulated signal is the cyclic autocorrelation function (CAF) from the previous chapter to detect its cyclic features. This method can be used in very noisy channels since noise does not have cyclostationary properties whereas (most) modulated signals have. Also, this feature doesn't need prior knowledge of phase and frequency offsets making it a good candidate for AMC. The theory of cyclostationary was treated in Chapter 3. Another statistical based feature is based on moments and cumulants. In Chapter 3, it was shown that both the theory of moments and cumulants, as well as some time domain features, can be viewed as a subset of the cyclostationary feature space.

4.3.2. Classifier Design

Depending on the extracted features, one has to choose how to classify a certain modulation type. In [7], two methods for the decision making after feature extraction are distinguished: Pattern Recognition (PR) and using a Decision Tree (DT). A well known example of the DT approach is given in [17]. A discrimination is made between modulation types based on the fourth order cumulants of the signal for different channel conditions. The critical part of this approach is to determine a threshold for every decision. This decision threshold can be obtained from theory, but it can also be determined using a training set. Using a training set to find a decision threshold is a form of machine learning. Some theory about machine learning in relation to signal identification will be treated in Section 4.6. A decision tree has the advantage of being easy to expand with more modulation types.

One example of the PR method is addressed in [14]. Figure 4.1 shows a block diagram of the method that is used for AMC. First the spectral correlation function (SCF) is calculated from the received signal as explained in Chapter 3. Than this information is transformed to a Cyclic Domain Profile (CDP) to reduce the information content. This is done by finding the maximum value of $S^{\alpha}_{yy^*}$ for every calculated value of α. At last, this CDP is compared with a predefined set of CDP's from known modulation types. The exact method for SCF calculation and CDP extraction is explained in the mentioned paper. However, one can further generalize this model by replacing the CDP extraction block by a general feature extraction block. In this manner, predefined patterns can be matched with all types of extracted features and not just the CDP features. These predefined patterns can be found in a theoretical way or by a training set (or a combination). This can be done by a form of machine learning which is explained in Section 4.6.

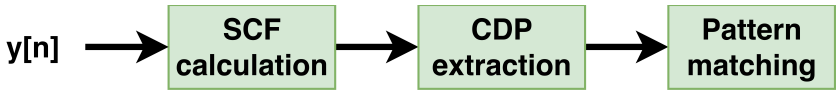

Figure 4.1: AMC based on pattern matching. The SCF is calculated from the received waveform $y[n]$. From this SCF the CDP is extracted. At last, this CDP is matched with templates of known modulation types.

From all these methods one wants to select the best one in terms modulation classification performance and minimal complexity. It is clear that there is no general approach, thus the methods that are best to the application must be selected. The next section gives two examples of modulation classification algorithms that can be found in literature. It will show positive and negative sides of these methods.

4.4. Digital Modulation Classification Using Cumulants

One of the ways that is extensively studied in literature to classify modulation types is based on stationary moments and cumulants. A well known example is addressed in [17]. A method is proposed to distinguish between modulation types based on fourth order cumulants. The performance of the classifier is presented for ideal conditions as well as under different channel conditions. This method can be seen as a stationary method. In other words, they do no exploit the cyclostationary properties of the modulated signal. This method demonstrates the ability to deal with non-ideal conditions: phase offsets, frequency offsets, different SNR's. A study was presented of the so called 4-class problem. A discrimination between four modulation types was made based on the absolute value of the fourth order cumulant C_{40}. This cumulant is defined as:

$$C_{40} = E\big[y[n]y[n]y[n]y[n]\big] - E\big[y[n]y[n]\big]E\big[y[n]y[n]\big] - E\big[y[n]y[n]\big]E\big[y[n]y[n]\big], \tag{4.9}$$

where the expectation operator is replaced by the sample mean if we have sampled data. The four modulation types are: BPSK, M-PAM, PSK>2 and M-QAM. This immediately shows that this method only works for a limited class of signals and requires that it is already known that the received signal uses one of these four modulation classes. For the exact details one can refer to [17]. This methods was tested in Gaussian noise channel. From Figure 4.2 one can see that we can distinguish between the indicated modulation types with a SNR > 10dB when we have only 192 samples.

However, testing their method clearly shows that the performance dramatically decreases if we analyse some more realistic scenarios. As we saw in Chapter 2, every real digital communication system has some kind of shaping filter to reduce adjacent channel interference and inter symbol interference. This results in a constellation plot without clear distinction of the IQ points due to smooth transitions between symbols. Since the cumulant method relies on this property of different modulation techniques (i.e. the difference in constellation) we can't use this method when pulse shaping is applied without any preprocessing. In this case, the performance can be improved by first finding the symbol rate. With knowledge of the symbol rate, the signal can be re-sampled so we will have a constellation with more distinct points. Another parameter that influences the constellation diagram is the carrier frequency offset. A frequency offset results in a clockwise (positive valued frequency offset) or counter clockwise (negative valued frequency offset) change of the constellation points making it impossible to use the cumulant method without preprocessing. However, if we are able to compensate for this offset we can still use this method. In conclusion, this is a low complexity method that only works for a limited number of modulation types and hardly any type of signal contamination. However, if we are able to do some preprocessing on the raw data, this method can be used under more realistic conditions. Coming back to the previous sections, this specific example is a statistical based method. The classifier that makes the actual decision about the modulation type is a Decision Tree based classifier.

4.5. Modulation Classification Based on a Cyclostationary Feature Vector

Another approach that can be used for modulation classification is based on exploiting the cyclostationary properties of a communication signal. For a more in depth discussion of cyclostationary signal processing one can refer to the previous chapter. However, we will shortly discuss this method to show its pros and cons. A well known method is based on finding the conjugate and non conjugate cycle frequencies [15]. Based on those cycle frequencies one can differentiate between modulation types. All digital modulated communication signals have cycle frequencies as a function of the symbol rate T_{sym} and carrier frequency f_c. With this method they can discriminate between M-ASK, M-PSK (M>2) and GMSK. Again, this method only works for a limited amount of modulation types. Furthermore, it has a higher complexity compared to the method from using cumulants. Its biggest advantage is the ability to deal with noisy channels as well as phase and frequency offsets. This method was tested under different channel conditions and this method completely depends on the ability to find the exact symbol rate and carrier frequency. Based on those two parameters, cycle frequencies α can be found that are unique for those three modulation classes. Looking at the theory

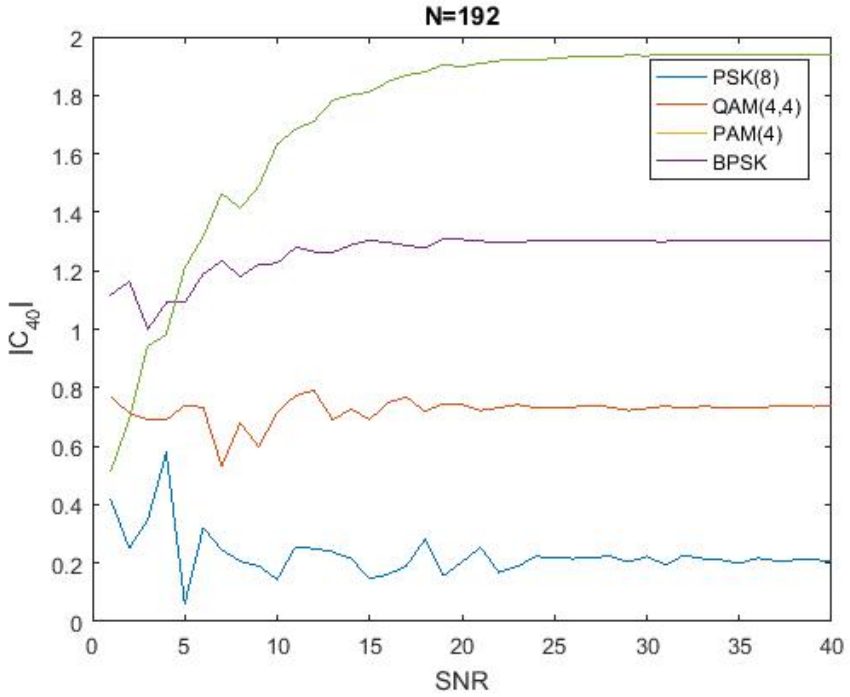

Figure 4.2: Cumulant value C_{40} of four modulation types is calculated as a function of the signal to noise ratio.

from this section, this method is again a (different) statistical based method. Furthermore, the actual decision is made by a pattern recognition classifier. So the calculated cycle frequencies are compared with a predefined set of cycle frequencies of known modulation types.

4.6. Machine Learning

The machine learning approach is an upcoming research area in the field of modulation signal classification which has gained a lot of interest in recent years. Within this research topic, algorithms are developed which allow a computer to learn to recognize patterns in data, rather than to have them recognize through explicit programming. This makes machine learning very interesting for applications in (amongst others) the field of pattern recognition, including modulation patterns.

Within the field of machine learning a distinction is made between two approaches, these being supervised and unsupervised learning. In supervised learning the objective of the machine learning algorithm is to find the optimal function which maps a number of inputs to a number of outputs, thereby providing a feedback mechanism which allows for the adaptation of the mapping function. In the unsupervised learning approach no feedback mechanism is present. Here the algorithm has to find its own structures and hidden patterns in the given data set.

One way of utilizing machine learning algorithms within the field of modulation classification relates to finding the optimal decision parameters given a number set of features derived from the sample data, such as cumulants and cyclostationary features [5]. Using this approach it is not necessary to determine the decision thresholds for each feature in each possible channel condition from theory. Rather, training datasets are used with known modulation types to train the algorithm and find the optimal weighting parameters.

The previous method relies on the completeness and performance of the provided feature set in order to find the optimal mapping function for classification. An alternative is the use of 'feature learning' algorithms. Here, the algorithm itself is responsible for finding the optimal feature set. Deep learning is a popular form of a feature learning method, for example through the use of convolutional neural networks (CNN) [11].

The drawback of the machine learning approach, as opposed to the decision tree method, is that the assump-

tion is implicitly made that a single feature set leads to the correct classification decision. This implies that every feature must be determined before the classification decision using the trained model, even though the calculation of more computationally intensive features may not be necessary.

Furthermore a great amount of training data is required to train the models. Especially in the case of the more exotic (and maybe therefore more interesting) modulation forms, little real world data may be available. One would therefore need to generate the training data set, thereby requiring knowledge of the modulation form itself.

Finally, the use of machine learning algorithms may further abstract the more in-depth understanding of how the features behave for different modulation forms in different channel conditions. Especially in the case of the feature learning approach where the resulting feature set can possibly be quite abstract and non-intuitive.

In conclusion, the potential of machine learning in relation to signal identification is recognized. However, it is not further researched in this project. It was preferred to develop a more in-depth understanding of how signal features can be extracted for different modulation types.

4.7. Comparsion Between Methods

From previous discussions, the conclusion is drawn that there is no general approach for the modulation classification of an unknown signal. LB methods for modulation classification will not be applicable in a blind scenario, because all unknown channel parameters have to be determined or estimated. FB methods turn out to have the most potential for modulation classification in a blind signal scenario. It was found out that those FB-methods related to modulation classification are hard to compare in terms of complexity and classification performance. Also, those classification algorithms can only deal with signals that are from a predefined set but lack the ability to deal with signal that are not from that set. Therefore, insightful knowledge of the unique characteristics of modulation types is needed to be able to deal with signals that are not from the set. This theoretical knowledge was already built in the previous chapter. In this chapter the statistical properties were defined and analysed in terms of complexity and performance. A distinction was made between stationary and cyclostationary features. Furthermore, in the more specific case of signal identification on a SDR platform, some prior knowledge is already available before the identification process starts. This prior information can then be used to improve or simplify the classification process. As stated in the introduction, a coarse estimate of the following features is available: bandwidth, center frequency, SNR and burst length. Now, by combining this prior knowledge with the insightful understanding of a modulated communication signal, identification algorithms will be developed.

5

Pre-processing for Blind Signal Identification

Generally speaking, if one is able to find the symbol rate, carrier offset and modulation type we can demodulate. After demodulation the data that was transferred can be analysed meaning that there is access to the raw transmitted data. Those 3 parameters of the unknown signal are therefore the most important ones. There are more parameters of the signal that are unknown, such as the exact parameters of the pulse shaping filter, but this is not researched.

If an SDR device is used, a coarse estimate of some parameters are already available. Those parameters are the SNR, bandwidth, carrier frequency and burst length. Those parameters can be used to reduce computational complexity for finding the modulation type, symbol rate and carrier offset. Furthermore, there are also some preprocessing steps that can be performed to simplify the identification process. One example is the process of amplitude scaling. Scaling the received signal in an early stadium will prevent scaling problems in later steps. For example, if a modulation type is classified based on the fourth order moment value the amplitude must be scaled to make a fair comparison between the calculated and theoretical value of this moment. The prior information given by the SDR must be combined with this preprocessing to find the best identification algorithms. This chapter describes the preprocessing steps.

5.1. Detection

In Chapter 1, the problem statement was defined and it was explained that the detection part will be neglected to narrow the project scope. However, we need knowledge of the detection performance and it's implications on later steps (i.e. blind signal identification). Therefore, this chapter will start with some basic detection theory. Detection and segmentation is the first step for the identification of a communication signal. Energy detection measures the energy received during an interval and compares it to a threshold. It is suitable for wide-band spectrum sensing [8]. In it's simplest form, we want to decide between the following two hypothesis:

$$\begin{aligned} \mathscr{H}_0 &: \mathbf{y} = \mathbf{n} \\ \mathscr{H}_1 &: \mathbf{y} = \mathbf{x} + \mathbf{n} \end{aligned} \tag{5.1}$$

The observations $\mathbf{y} = [y[1], y[2], .., [y[n]]$ are used to decide whether a signal $\mathbf{x} = [x[1], x[2], .., [x[n]]$ is present in the presence of noise $\mathbf{n}$. Now the energy under both hypotheses can calculated and compared to a certain threshold:

$$\hat{\Omega} = \begin{cases} \mathscr{H}_0, \text{if} & |\mathbf{y}|^2 < \lambda \\ \mathscr{H}_1, \text{if} & |\mathbf{y}|^2 > \lambda \end{cases} \tag{5.2}$$

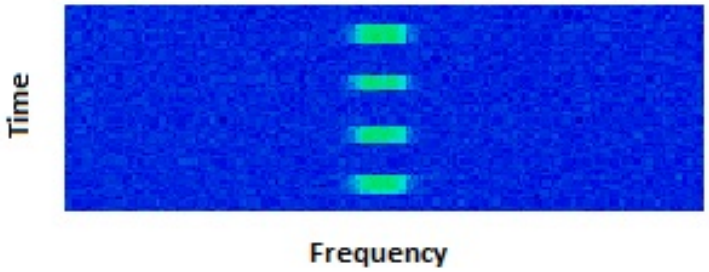

(a) Spectogram of an unidentified transmitter

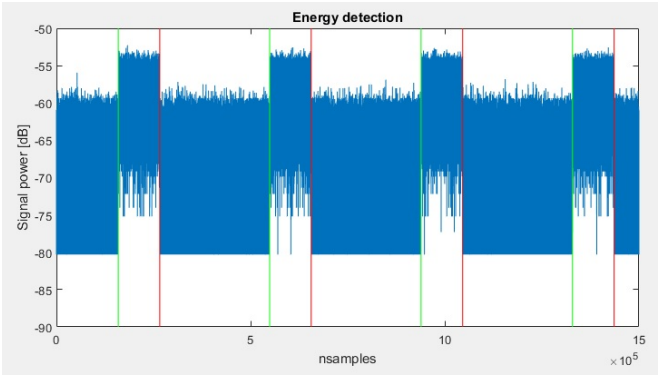

(b) Energy detection performed on an unidentified transmitter. The part of the signal between the green and red line are above some predefined threshold λ

Figure 5.1: Working principle of energy detection applied on a unidentified transmitter.

The threshold λ is chosen such that it satisfies a predefined false alarm probability by using the (estimated) noise distribution. When the probability density functions under each of the hypotheses are perfectly known, the energy detector performs close to optimal [2]. Figure 5.1 shows a spectrogram of some unidentified transmitter that is picked up with a SDR device. The exact parameters used are not important but it's to show the working principle of energy detection.

Fundamental limits for detection arise when operating at low SNR's or when the noise variance is unknown. Setting the threshold $\hat{\Omega}$ that is based on an incorrect estimation of the noise distribution degrades the performance significantly[18]. Refering to Figure 5.1, this means that if we set the threshold to -50dB those signals will not be detected. An adaptive estimation of the noise power and distribution is proposed in [12]. Also finding narrow-band signals in a wide-band environment gives rise to a challenge. The computational complexity of detection must be low in order to process all communication signals in a dense signal scenario. Communication signals with overlapping frequency spectra should ideally be separated as well. All these challenges regarding energy detection are well summarized in [18].

Another approach for detection could be to use the cyclostationary properties of a communication signal. It could be used for both blind and non-blind signal identification. In this case, non-blind means that we can correlate a feature of the signal with a signal from a database. Coming back to the example of GSM from the introduction, we know that we can expect that signal in the 900 MHz frequency band. The cycle frequencies of this signal are known beforehand. So we can correlate this knowledge of the incoming signal to see if the signal is actually present. In the case of blind signal identification we can't match this information about cycle frequencies with known cycle frequencies. However, the presence of a signal at non-zero cycle frequencies is a good indication for the presence of a communication signal. It can therefore be used as a blind detector. The cyclostationary detector can be used even for signals below noise level since it can still find cycle frequencies as an indication of signal presence. The detection of DSSS (Direct Sequence Spread Spectrum) without prior knowledge could therefore be done by exploiting the fluctuations of autocorrelation estimators. Those are different for white noise and a DSSS modulated signal below the noise floor [3]. It

turns out to be a very computational expensive operation especially when searching for a DSSS signal below noise level in a wide frequency band. FHSS (Frequency Hopping Spread Spectrum) modulated signals can be detected with energy detection. The challenge will be to detect frequency agile short time signals when they are operating in a wide spectrum band. Again the detection of signals in a wide-band scenario is outside the scope of the project.

5.2. Signal to Noise Ratio

Another useful parameter that can be used that is easily estimated is the signal to noise ratio. In [13], an overview is provided of SNR estimation techniques. An important distinction is made between two different estimators: data-aided and non-data-aided estimators. Data-aided estimators use knowledge of the transmitted signal whereas non-data-aided estimators only use the received signal. Clearly, a non-data-aided estimator must be chosen since there is no knowledge about the transmitted signal. As we see later, different identification techniques are more vulnerable to a low SNR. So if we have a high SNR, a lower complexity algorithm can be chosen, whereas with low SNR a computationally more expensive algorithm can be used. We don't need exact knowledge of the SNR, but even a coarse estimate could reduce complexity. Furthermore, the SNR can be used to optimize the threshold in a certain decision step. In Chapter 6 an example will be shown where the threshold is adaptively changed based on the SNR. The theory for the exact determination of he SNR will not be treated in this report. So we assume that before the blind identification starts, there is a coarse estimate of the SNR.

5.3. Bandwidth and Pulse Shaping Filter.

In communications systems all signals must be band limited to prevent adjacent channel interference (ACI). This means that the out-of-band power must me minimized to prevent interference between communication systems that operate in frequency bands close to each other. In real systems this is achieved by using a pulse shaping filter before actual transmission of the waveform. This pulse shaping filter also results in smoother transitions between symbol states making it harder to distinguish between modulation types. A pulse shaping filter is also a feature of a communication signal, but it's hard to find it's exact parameters in a blind signal scenario. We must however know it's implications on the identification performance and some theory will therefore be treated in this chapter. A frequently used pulse shaping filter is the root raised cosine (RRC) filter. The relation between symbol rate T_{sym}, filter bandwidth B and roll of factor β is given by:

$$T_{sym} = \frac{(1+\beta)}{2B}, \tag{5.3}$$

Where the roll of factor must be in the interval $[0,1]$. Figure 5.2 [1] shows the time and frequency domain response of a raised cosine filter for different roll of factors β. Two root raised cosine filters combined results in the same response as a raised cosine filter. A root raised cosine filter is therefore used to have one at the transmitting side and one at the receiving side of a communication link. From the impulse response, it can be seen that this filter can eliminate inter symbol interference (ISI), because the impulse reponse is zero at all nT_{sym}, where $n = [1,2,..]$ and T_{sym} is the symbol rate. The frequency response of the raised cosine filter shows that the bandwidth will be between $2/T_{sym}$ and $1/T_{sym}$, depending on the roll of factor of the filter. Figure 5.3 clearly shows the effect of the raised cosine filter for a QPSK signal with frequency bands close to each other. Generally, in communication systems, bandwidth is defined as the point where the frequency spectrum is decreased by 3dB. This can be found by the Fast Fourier transform of the time domain signal and find the -3dB point. When a communication signal is digitized you have to deal with effects like quantization noise directly resulting in a estimation error. Furthermore, applying a DFT on the data will implicitly influence the -3dB point since it depends on factors like window length, the chosen windowing function and number of overlapping samples. All these effects will affect the estimation accuracy of the bandwidth. Another possible limiting factor would be peaks or dips in the frequency spectrum bigger than 3dB. This will result in a false separation of signals. A solution must be found for this problem. However, as stated in the introduction, this project assumes that the received IQ-data contains just 1 signal so we don't have to deal with this special case. From the previous we conclude that the bandwidth can be roughly estimated. This bandwidth is a feature that can distinguish between communication signals. An advantage of bandwidth estimation is the possibility to use it as an order of magnitude estimator for the symbol rate in later steps. This will reduce computational complexity. Depending on the exact modulation type, the relation between symbol rate and bandwidth is

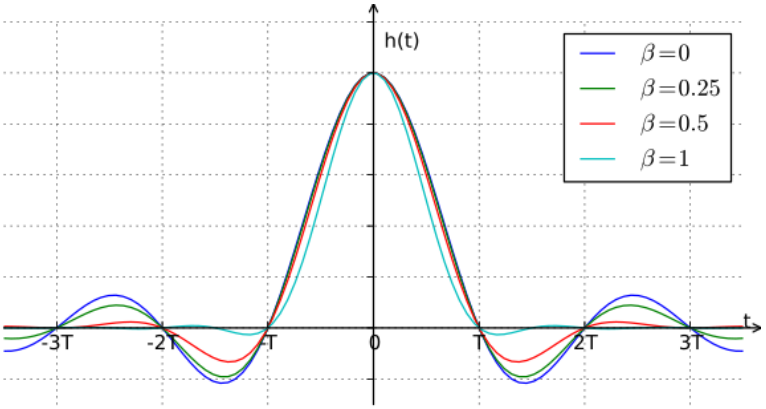

(a) Impulse response of a raised cosine filter for different roll-off factors β. It can be seen that ISI is removed due to zero crossings at multiples of the symbol rate.

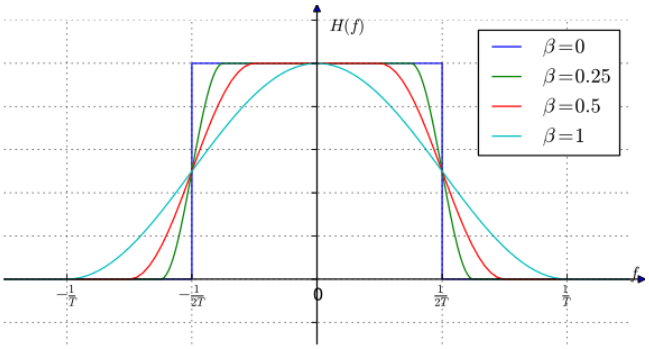

(b) Frequency response of a raised cosine filter for different roll-off factors β

Figure 5.2: Impulse and frequency response of a raised cosine filter..

different. The influence of a pulse shaping filter on the classification algorithms will be presented in Chapter 6 and Appendix A, where a worked out example of QPSK is presented.

5.4. Continuous and Burst Signals

A feature of a communication signal that is easily derived is it's presence in the electromagnetic spectrum over time. The first step would be the discrimination between continuous and burst signals. An example of a communication signal that is continuously present in the electromagnetic spectrum is FM radio. If we identify a communication signal as a burst signal we could check if this signal appears just once in the spectrum or if it's a repeating occurrence. For example, some FHSS protocols change their carrier frequency with a repeating sequence. This sequence of carrier frequencies could be an unique feature of a communication signal. Under the assumption that only one signal is present in each sample data set the presence of a burst signal implies a need to be able to identify multiple datasets as being part of the same signal. This is however not researched.

5.5. Resampling

An important step that directly decreases computational complexity is the process of re-sampling. With the knowledge of the signals bandwidth we can already make a coarse estimate of the symbol rate. According to [10], the oversampling factor to do cyclostationary analysis of a communication signal must satisfy $P > 4$, where $P = T_{sym}/T_s$. Referring to section 5.3, we know that the relation between bandwidth and symbol rate satisfies $1/B > 2T_{sym}$. This means that the received waveform must be sampled with at least $8B$. For now we take the oversampling factor as a constant value of $P = 10$.

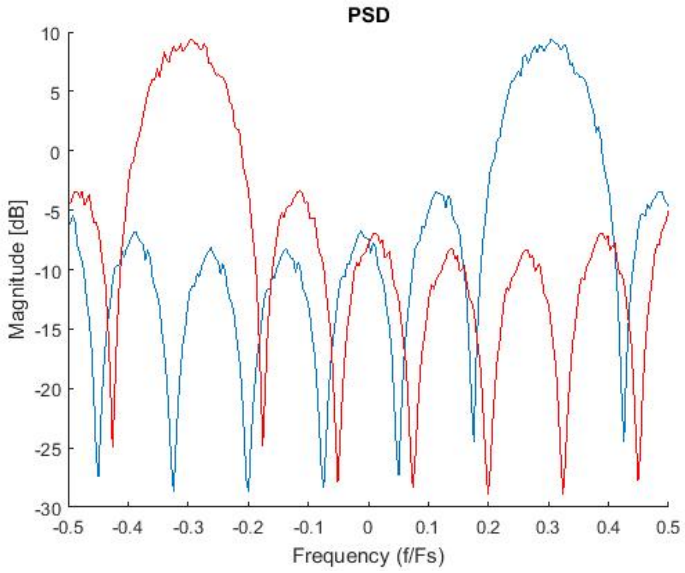

(a) No shaping filter before transmission

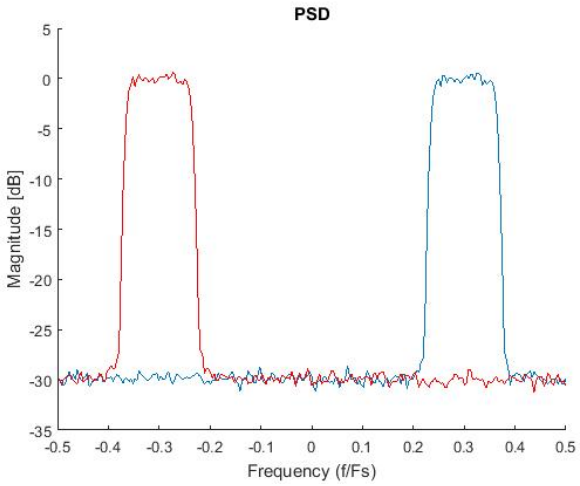

(b) Root raised cosine filter used before transmission with a roll of factor $\beta = 0.2$ and 10 filter taps.

Figure 5.3: This figure shows the working principle of a pulse shaping filter used before transmission. In both figures, the red line represent a QPSK signal with a carrier frequency (relative to the sampling frequency) of -0.3 wheras the blue line has a carrier frequency of 0.3. It shows that the use of a shaping filter reduces interference between signals with a center frequency close to each other.

5.6. Amplitude Scaling

After re-sampling, amplitude scaling is applied to the received waveform. This can either be done in software or hardware. In the practical case when using a SDR, this is done in software by an Automatic Gain Control. This will prevent scaling problems in later steps. An AGC is a feedback loop that tries to provide a constant output power while the input power can change over time. So the received waveform ideally has unit energy, but it practice we'll still have fluctuating signal power. This will reduce the performance of the identification algorithms. The parameters of a software based AGC are the adaptation step size, the desired output power and the averaging length. We can also limit the output power gain, which prevents problems if the signal power rapidly increases in a short period. The adaptation size is a trade off between adaptation speed when we have fast variation of signal power and higher variation in the output power in static operation. The averaging length is the number of samples used for the averaging window. The chosen parameters depend on the scenario at hand. M-ASK and M-QAM modulated signals have a changing amplitude in it's carrier to transfer information. This could give problems when using an AGC, since it wants output a signal with constant amplitude. It must be noted that fluctuating signal amplitude will reduce identification performance. Methods from the LOS and HOS framework are most vulnerable to fluctuating signal amplitude, because the resulting statistics are directly related to this amplitude. In contrast, methods from the SOCS and HOCS framework are generally less vulnerable to fluctuations. This is because we are searching for locations of cycle frequency α. So not the exact amplitude of the peak at a specific cycle frequency is the most important. An AGC dynamically adjusts the gain to provide constant output power. However, for now it was assumed that we have a constant energy for the complete sample size N. Therefore we can apply scaling such that the received signal has unit energy meaning that:

$$\frac{1}{N}\sum_{n=1}^{N-1}|y[n]|^2 = 1 \tag{5.4}$$

6

Building a Decision Tree

In Chapter 3, it was explained how a communication signal can be statistically described. In general, this can be done as time domain (cyclo)stationarity and frequency domain (cyclo)stationarity. The complexity of those methods is explained as well. Furthermore, in Chapter 5 it was shown which information is known at the start of the identification process. The available parameters are a coarse estimate of the bandwidth, SNR, carrier frequency and burst length. This prior information is presented, together with some preprocessing steps. By using those statistical descriptions and combining these with the known parameters of the signal, low complexity algorithms are developed for the identification process. By also performing preprocessing, as explained in Chapter 5, the identification performance will be further improved.

In the introduction we limited ourself to digital single carrier modulated signals. We further generalize this by focussing on the following modulation types: ((G)MSK M-FSK, BPSK, M-PSK, M-QAM, M-ASK, M-PAM and OQPSK), where M is the modulation order. OQPSK is not stated as a subset of QPSK. The reason is that the identification process for QPSK and OQPSK is different as we will see later in this chapter. Those are the main classes of single carrier digital modulated signals. To test the algorithms, presented in this chapter, under some realistic conditions, the non-constant envelope modulated signals (BPSK, M-PSK,M-QAM,M-ASK, M-PAM and OQPSK) are simulated with the use of a transmit filter. The transmit filter used is the root raised cosine filter. See Chapter 5 for a detailed explanation. The roll-off factor $\beta = 0.2$ and filter length $l = 10$ are chosen to have a good compromise between minimizing inter-symbol interference and filter length. In a practical situation, the exact parameters of the transmit filter are unknown. However, a changing roll-off factor mainly reduces the amplitude of the peaks at cycle frequency α when doing a cyclostationary analysis. This is further explained in Appendix A for a QPSK modulated signal. In the proposed algorithms, not the amplitude of these peaks are the most important, but the locations. Those locations will not change with different roll-off factors β so therefore the algorithms are tested with a constant roll-off factor. MSK and GMSK modulated signals naturally have their own pulse shape. The simulated FSK modulated signals will not be pulse shaped before transmission.

Now, based on the developed work from previous chapters, a decision tree will be proposed in this chapter. To develop the best algorithms, to find the wanted features (modulation type, carrier offset and symbol rate), we must acknowledge the unique characteristics of every modulation type. This generally means that we are exploiting the phase, amplitude and frequency information from the unknown signal. First, we want to use low cost algorithms (stationary) to discriminate between modulation classes by exploiting those unique characteristics. Second, more complex (cyclostationary) algorithms will be used to either deal with low SNR signals or to distinguish between higher order modulations that have similar statistical properties. The difference between 'high SNR' and 'low SNR' will be explained in the next sections.

6.1. Constant/Non-constant Envelope Modulation

The received signal, that is already re-sampled and scaled to have unit amplitude, can either be a constant envelope modulated signal, or a non-constant envelope modulated signal. This distinction is important, because non-constant envelope modulated signals can be distinguished based on there constellation diagram

i.e. their phase and amplitude information. In contrast, the constant envelope modulations can't be distinguished based on their constellations. If phase modulated signals are oversampled we will have transitions between different symbols resulting in amplitude fluctuations. Amplitude modulated signals naturally have a fluctuating amplitude. These fluctuations can therefore be used to discriminate. The non-constant envelope modulated signal that is the most critical one is OQPSK. This modulation type does not have large amplitude fluctuations. This is the result of a $T_{sym}/2$ shift between the in phase and quadrature meaning they will not change at the same time. In other words, standard QPSK can have phase transitions of π whereas OQPSK can have phase transitions of at most $\pi/2$. Large phase transitions results in more amplitude fluctuations. So if we are able to distinguish between OQPSK and any other constant envelope modulated signal, this method will works for any other non-constant envelope modulated signal. Amplitude fluctuations can be found by:

$$\gamma_{max} = max|DFT(A_c)|^2/N, \tag{6.1}$$

Where $A_c[n]$ is the centralized version of the amplitude $A[n]$ of the unknown signal. It is centralized according to $A_c[n] = A[n] - 1$. This centralization is done because now the amplitude fluctuates around zero. In other words, it does not have a DC-component which would result in a large peak in it's frequency spectrum. The Discrete Fourier Transform (DFT) is thus calculated to show the amplitude fluctuations. This method is a transformation based lower order statistic (LOS) which as explained in Chapter 3. A complexity analysis of this method can be found as well.

Another way to discriminate between constant envelope and non-constant envelope modulations is to look at the standard deviation of the absolute value of the centred instantaneous amplitude:

$$\sigma_{aa} = \sqrt{\frac{1}{N}\Big(\sum_{n=1}^{N} A_c^2[n]\Big) - \Big(\frac{1}{N}\sum_{n=1}^{N} |A_c[n]|\Big)^2}, \tag{6.2}$$

where the standard deviation σ_{aa} is calculated for the centred amplitude A_c from the received waveform. This methods also describes the amplitude fluctuations around DC. This method is from the time domain LOS framework. Figure 6.1 shows the value of γ_{max} as a function of the SNR for four modulation types. One wants to discriminate between signals from the set (QPSK,OQPSK) and (FSK,GMSK). It can be seen that a threshold can be chosen at every SNR to make this distinction. In other words, if the threshold is adaptively changed according to the (known) SNR value, a reliable decision between constant envelope and non-constant envelope modulated signals can be made.

Figure 6.2 shows the resulting value for σ_{aa}, again as a function of the SNR, for the same four modulation types. Again, if the threshold is set adaptively as a function of the SNR, a reliable discrimination can be made. If now both algorithms are compared in terms of complexity, the function for σ_{aa} will be preferred. This follows from Chapter 3 where is described that functions from the time domain LOS framework are less complex than functions from the spectral based LOS framework.

6.2. Non Constant-Envelope

6.2.1. Carrier Offset Estimation and Compensation

After a positive match on a non-constant envelope modulation type we will start by calculating the carrier frequency offset. We need this parameter if we want to demodulate, but it can also be used to pre-process the data before the modulation type is classified. Therefore, it was chosen to first calculate and compensate for this frequency offset.

The down-mixing to baseband by the SDR results in a coarse estimate of the carrier frequency. From previous chapters we know that the down mixing will never be perfect, but has some residual carrier offset. If we have knowledge of the tolerance of the SDR device in estimating the carrier frequency, we can use this information to reduce complexity and evaluate for a limited values of cycle frequency α. However, we assume there is no

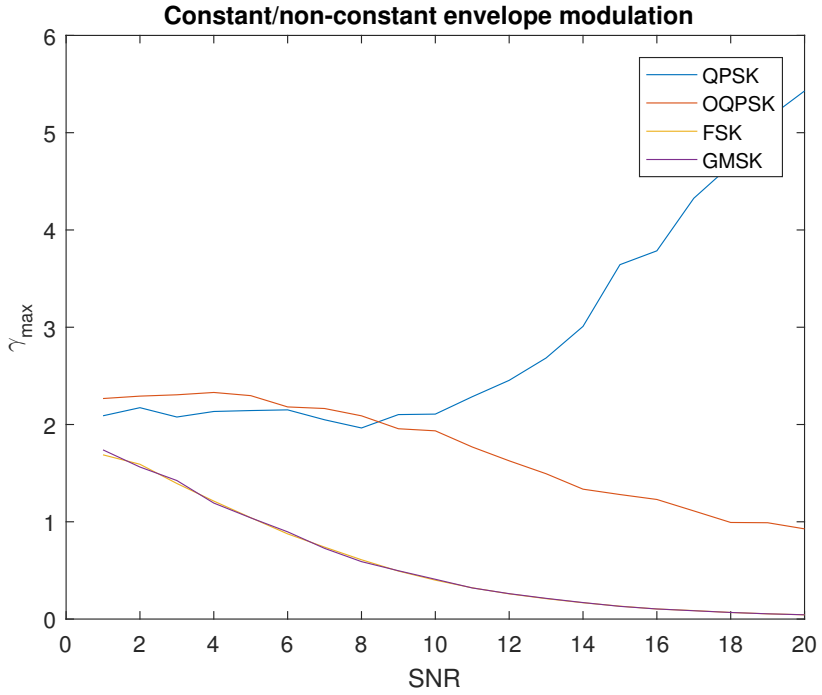

Figure 6.1: γ_{max} for a different SNR, $T_{sym} = 10T_s$. Every SNR is simulated and averaged over 100 calculated values of the SNR. The number of samples N=5120

knowledge about this tolerance. Therefore, we search for cycle frequency $\alpha = 4fc$ from the set $-0.5 < \alpha < 0.5$. The upper and lower limit is to prevent aliasing. In other words, we must make sure that the coarse estimate of the carrier offset is within $f_0 < 0.125\alpha$, which is easy realizable in practice. The function that is evaluated to find α is given by:

$$R^{\alpha}_{yyyy}[n, \tau = \mathbf{0}] = \sum_n y^4[n] * e^{(-i2\pi\alpha n T_s)} \tag{6.3}$$

This methods is in the HOCS framework, evaluated for a constant delay vector $\tau = [\tau_1, \tau_2, \tau_3, \tau_4] = [0,0,0,0]$. In Appendix A this is theoretically shown for a QPSK modulated signal. The first coarse estimate of the cycle frequency can be used to set a search window W_{f_c} for the following optimization problem

$$\max_{\alpha_i \in W_{f_c}} \left| \sum_{n=0}^{N_{f_c}-1} |y[n]|^4 e^{-i2\pi\alpha_i n T_s} \right|, \tag{6.4}$$

where we search for the cycle frequency $\alpha = 4f_o$ that is in the window W_{f_c}. A finer resolution of α is thus chosen to get closer to the true value. This is graphically shown by Figure 6.3a and Figure 6.3b. A frequency offset of $f_o = 0.01$ was chosen so we are searching for a cycle frequency $\alpha = 4f_o = 0.04$. First a coarse estimate was done to approximately find the offset. Then a finer resolution for α was chosen getting closer to the true value.

This estimation method works for almost any digital linear modulation type (ASK, M-QAM, M-PAM, M-PSK M<8, OQPSK). It does not work for M-PSK with order M≥ 8. The reason is that if the fourth power of an 8-PSK signal is calculated, the phase information is not removed. Therefore the fourth power of a 8-PSK signal does not only have frequency information but also consists of phase information. In practice, most PSK modulated signals in wireless communications have order lower then 8. However, by slightly adapting Equation 6.3 we can still find this frequency offset if needed. This can be done by solving the following problem:

$$R^{\alpha}_{y^M}[n, \tau = \mathbf{0}] = \sum_n y^M[n] * e^{(-i2\pi\alpha n T_s)} \tag{6.5}$$

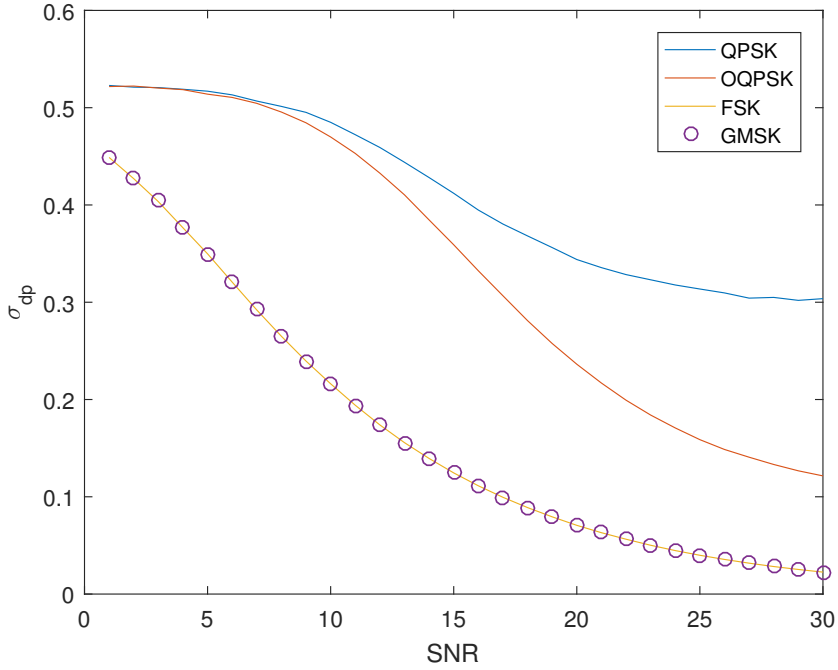

Figure 6.2: σ_{aa} for a different SNR, $T_{sym} = 10T_s$. Every SNR is simulated and averaged over 100 calculated values of the SNR. The number of samples N=5120

Where we search for the cycle frequency $\alpha = M * f_o$, where M is the modulation order. So in a real system we start with a search for a peak at cycle frequency $\alpha = 4f_o$. If we cannot find a peak at that cycle frequency the order can be increased to search for peaks. The same optimization problem from Equation 6.4 can be used to get closer to the true value. However, with increasing order the chance for aliasing will increase. For example, if we have PSK with order 16 the frequency offset (relative to the sample frequency) must be $f_0 < 0.5/16\alpha$ which however is still easy realizable in practice. The frequency can now be compensated by multiplying the original received waveform $y[n]$ with the following complex exponential:

$$y_{comp}[n] = y[n]e^{i(2\pi f_o n T_s)} \tag{6.6}$$

6.2.2. ASK/Non-ASK Distinction

When the frequency offset is compensated, we can use another low complexity LOS to distinguish between ASK and non-ASK modulated signal. An ASK modulated signal is the only digital single carrier modulated signal that does not have phase information in it's carrier. This observations can be used to distinguish between ASK and non-ASK modulated signals in a early stage of the proposed decision tree. The method from the LOS framework that is used is the standard deviation of the absolute value of the instanteneous phase and described as [22]:

$$\sigma_{dp} = \sqrt{\frac{1}{N_c}\Big(\sum_{A_n[n]>A_t} \Phi^2_{NL}[n]\Big) - \Big(\frac{1}{N_c}\sum_{A_n[n]>A_t} |\Phi_{NL}|\Big)^2}, \tag{6.7}$$

where N_c is the number of samples that meets the condition $A_n[n] > A_t$. The threshold A_t makes the value of σ_{dp} less sensitive to signals with low amplitude. Figure 6.4 shows a scatterplot of an ASK modulated signal. The red circle represents the threshold A_t. If only signals that meets the condition $A_n[n] > A_t$ are considered, the standard deviation of the phase will be much lower. The term Φ_{NL} represents the instantaneous phase.

Figure 6.5 shows the resulting plot for σ_{dp} as a function of the SNR. One can set a constant threshold of $\sigma_{thres} \approx 1.55$. The reliability can be increased if the threshold adaptively changes with changing SNR. This

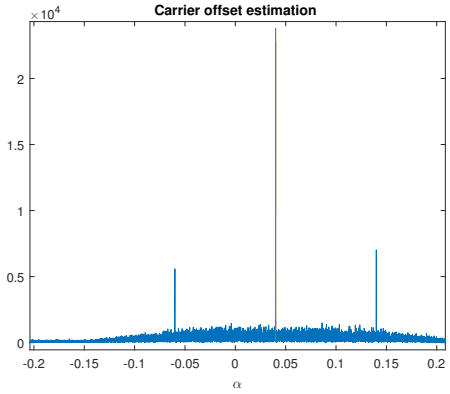

(a) QPSK modulated signal, where the function is evaluated for $< -0.2\alpha < 0.2$

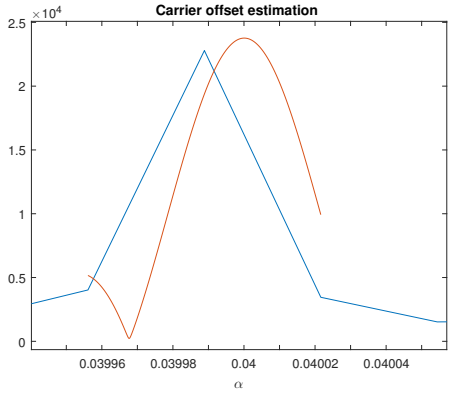

(b) QPSK modulated signal, where the function is optimized around the first coarse estimate of the frequency offset

Figure 6.3: QPSK modulated signal, with N=5120, $T_{sym} = 10T_s$. The blue line represents the first coarse offset found by the function $R^{\alpha}_{yyyy}[n, \tau = \mathbf{0}]$. The red line represents the optimized carrier offset estimation by choosing a finer resolution in α.

method has good performance, even in low SNR regions. The key in this decision step is the removal of the frequency offset because a frequency offset adds phase information to the ASK modulated signal.

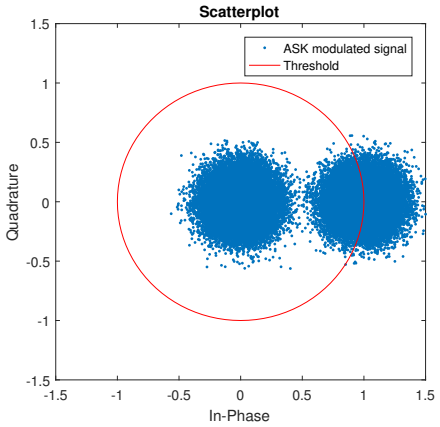

Figure 6.4: Scatterplot of an ASK modulated signal with SNR=8dB. Only signals with amplitude $A[n] > 1$, so outside the red circle, will contribute to the standard deviation of the phase.

6.2.3. OQPSK/non-OQPSK Distinction

If a signal is classified as a constant envelope modulated signal and as s non-ASK modulated signal we are left with signals from the set (BPSK, M-PSK, M-QAM, M-PAM and OQPSK). First the OQPSK signal will be separated from the other signals from the set. This step is important, because determining the symbol rate for OQPSK is different then for other digital single carrier modulated signals [9]. A method from the SOCS framework can be used to make this discrimination. A signal that is OQPSK modulated does not have cycle frequencies as a function of the symbol rate T_{sym} in the CAF. This is due to the offset of $T_{sym}/2$ between the in phase and quadrature components.

The conjugate CAF has the ability to discriminate between OQPSK and non-OQPSK modulated signals. OQPSK is the only constant envelope modulated signal that has cyclic frequencies α at $[\frac{-1}{2T_{sym}}, \frac{1}{2T_{sym}}]$ in the conjugate CAF. This conjugate CAF from Chapter 3 is given by:

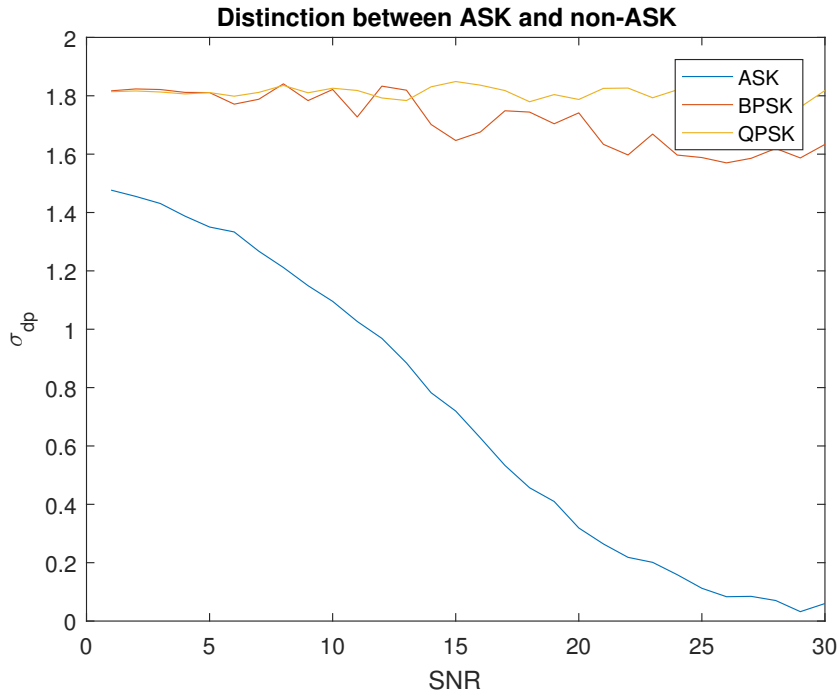

Figure 6.5: Threshold At=0.9, phase $\phi[n]$ varies randomly between 0-360 degrees. N=5210 sample.

$$R_{yy}^{\alpha}[n,\tau] = \sum_{n=0}^{N-1} y[n+\tau_1]y[n+\tau_2]e^{-i2\pi\alpha nT_s} \tag{6.8}$$

Figure 6.6 shows this function evaluated for lag parameter $\tau = 0$ for three different modulation types. One can see two clear peaks at $\alpha = -0.05$ and $\alpha = 0.05$ for the OQPSK modulated signal. Therefore this method has the ability to distinguish between OQPSK and non-OQPSK modulated. A huge advantage is that the spacing between the two α peaks directly gives an estimate of the symbol rate. How this coarse estimate can be refined will be explained in the next section. Thus after a positive match on OQPSK, both the carrier offset and symbol rate are known meaning the signal can be demodulated.

6.2.4. Symbol Rate Estimation.

After detection and separation we will have a coarse estimate of the bandwidth information. This information can then be used as an order of magnitude estimator of the symbol rate. The bandwidth of the unknown signal can be estimated as described in Chapter 5. The relation between bandwidth B and symbol rate T_{sym}, for RRC filter, is given by:

$$T_{sym} = \frac{(1+\beta)}{2B}, \tag{6.9}$$

where β is in the interval $[0,1]$. The symbol rate can be calculated by a SOCS operation, where we can reduce complexity by evaluating the function for 1 delay value τ. To extract the symbol rate we will perform the following operation (by using bandwidth information):

$$\max_{\alpha_i \in W_T} \left| \sum_{n=0}^{N_T-1} |y[n]|^2 e^{-i2\pi\alpha_i nT_s} \right| \tag{6.10}$$

where the number of samples N_T and the cyclic frequency α_i is chosen such that it fulfils the condition $0 < N_T * \alpha_i = W_T < 1/2B$. The resulting cycle frequency α gives a coarse estimate of the symbol rate. This can

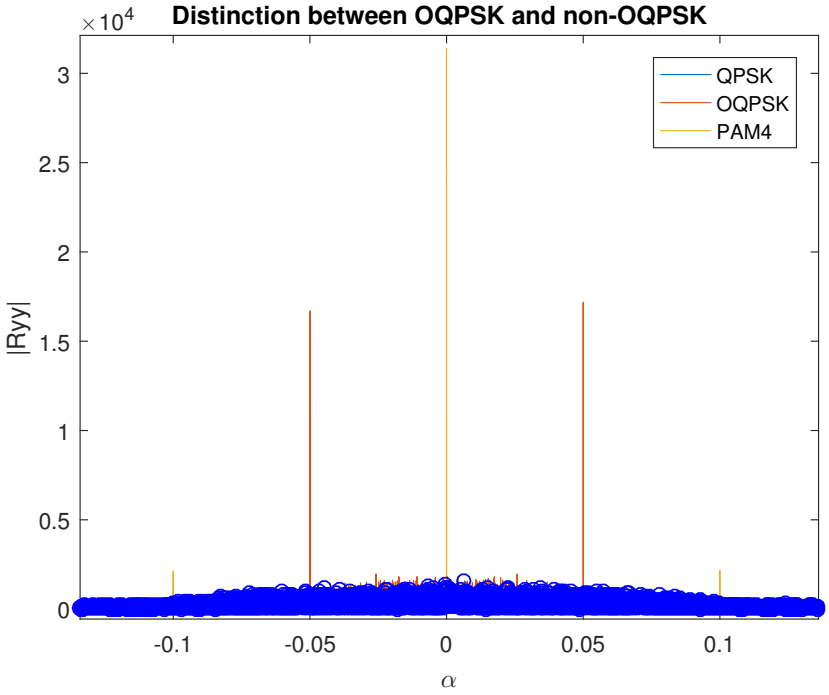

Figure 6.6: Conjugate cyclic autocorrelation function for three different modulated signals. SNR=10, N=51200

be further optimized by doing the same operation , but with smaller step-size α. This results in the following optimization problem:

$$\max_{\alpha_i \epsilon W_{T_r}} \left| \sum_{n=0}^{N_{T_r}-1} |y[n]|^2 e^{-i2\pi\alpha_i n T_s} \right| \tag{6.11}$$

where $T_{sym} - \epsilon < N_{T_r} * \alpha_i = W_{T_r} < T_{sym} + \epsilon$. This results in an estimate of the symbol rate $\alpha = T_{sym}$ with a higher resolution. The value of ϵ is chosen according to the resolution chosen in Equation 6.10. This method works for any non-constant envelope modulated signal from the set (M-ASK, M-PSK, M-QAM, M-PAM) except for OQPSK, which is explained in the previous section. This methods has a trade-off between number of samples and the SNR. If we are in a low SNR region more samples are needed to have a clear peak at cycle frequency $\alpha = 1/T_{sym}$. It was assumed that the number of samples is not the limiting factor, making this method a reliable estimator for the symbol rate.

6.2.5. Decision Based on SNR

The SNR is the most limiting factor for the modulation classification algorithms. In the previous sections, it was found out that reducing the set ((G)MSK M-FSK, BPSK, M-PSK, M-QAM, M-ASK, M-PAM and OQPSK) to the set (BPSK, M-PSK, M-QAM, M-PAM) can be done with an SNR as low as 5dB.

The signals from the set (BPSK, M-PSK, M-QAM, M-PAM) can be distinguished in different ways based on the SNR. Depending on this SNR, different algorithms will be chosen. We use this approach to reduce complexity. Cyclostationary methods are more robust against low SNR-regions, whereas stationary methods needs higher SNR. In other words, if classification can be done based on the constellation diagram (i.e the distribution of the in phase and quadrature) we use stationary methods. If this is not possible, cyclostationary methods are used. The SNR threshold can be based either on theory as well as on a training set (machine learning).

To show the reliability of the stationary methods, some cumulants are tested as a function of SNR and compared with it's theoretical values. The cumulants C_{40} and C_{42} are chosen because those are well described in literature. Furthermore, they can be used to discriminate between four modulation types. Therefore those two cumulants are used because they clearly point out the performance of stationary methods. Table 6.1

	C_{40}	C_{42}
BPSK	-2.0	-2.0
QPSK	1.0	-1.0
QAM16	-0.68	-0.68
PAM4	-1.36	-1.36

Table 6.1: Theoretical values for stationary cumulants for 4 different modulation types.

shows the theoretical values of cumulants C_{40} and C_{42} from the HOS framework from Chapter 3. The theoretical values of those cumulants are similar for the four indicated modulation types, excepts for QPSK. However, both cumulants are still tested for all four different modulation types because they are found by a different non-linear operation as explained in Chapter 3 making it an extra check of the performance of a cumulant method.

The theoretical values were compared with simulations with four different modulation types having a frequency offset. This offset was first compensated. Then the symbol rate is estimated and the received signal is resampled accordingly. From the resulting complex data the cumulant values are calculated. The results are shown in Figure 6.7 and Figure 6.8. One can see that if the SNR increases the values will converge to the true value. For this specific example one can set a threshold for an SNR higher than ≈ 20. Also different order moments and cumulants were tested. It was found out that generally the SNR of around 20 is the point were the values are close to the true value.

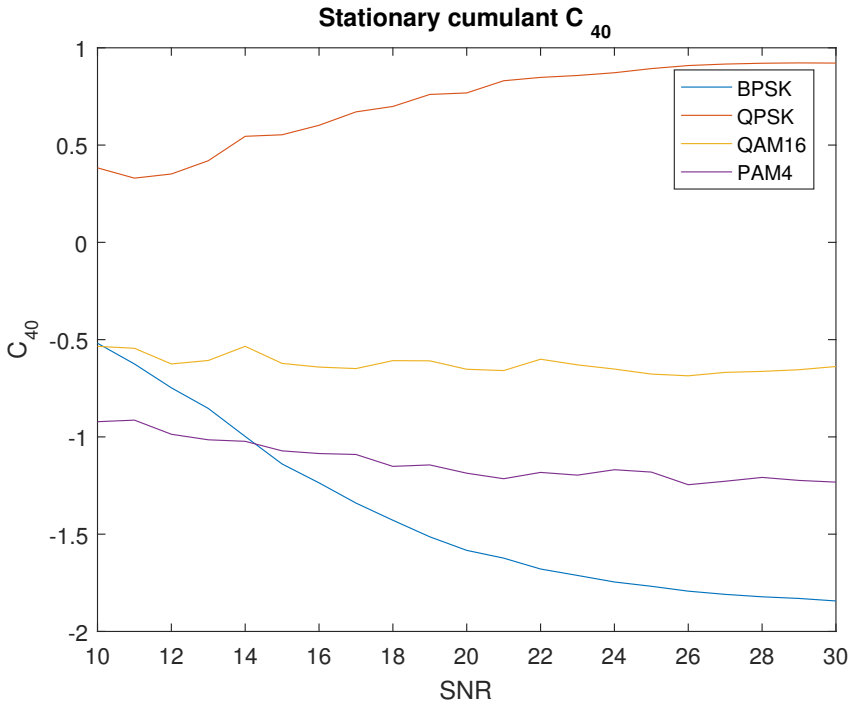

Figure 6.7: Cumulant value C_{40} as a function of the SNR. The frequency offset was calculated and compensated accordingly. The symbol rate was estimated as well. Original signal length N=51200. After resampling the number of samples equals 5120 (T_{sym}=10T_s)

To distinguish between modulation types based on their (higher order) cyclostationary properties requires more computations as explained in Chapter 3. To reduce this complexity, we first have to estimate the second order cycle frequencies as a function of the symbol rate T_{sym} and the carrier offset f_o. The estimation of these cycle frequencies is already done in previous steps. The search for cycle frequencies within the higher order cyclostationary framework can then be done to discriminate between modulation types in a low SNR region. At this point in the proposed decision tree, carrier offset estimation and compensation is already

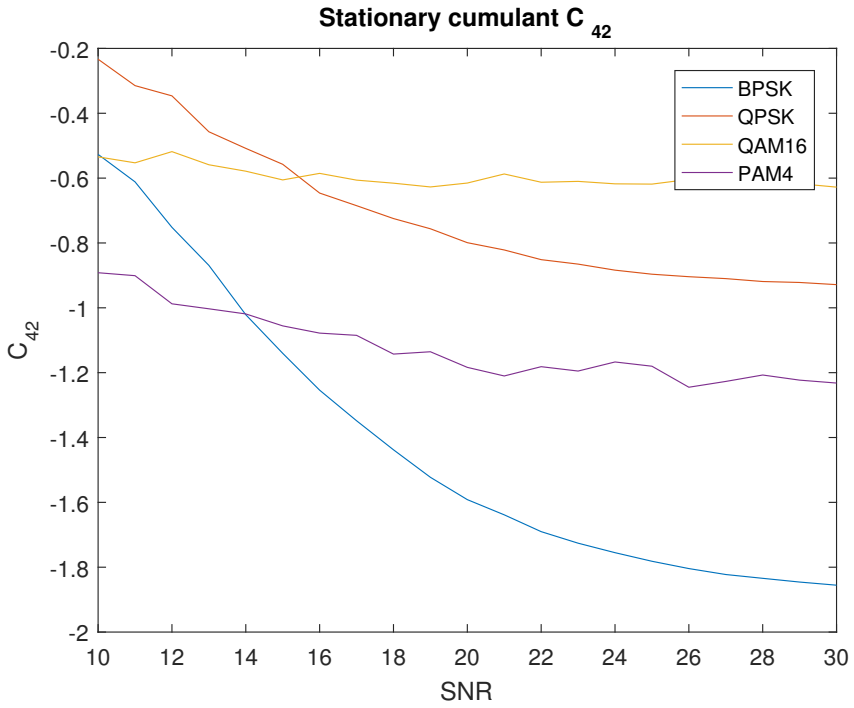

Figure 6.8: Cumulant value C_{42} as a function of the SNR. The frequency offset was calculated and compensated accordingly. The symbol rate was estimated as well. Original signal length N=51200. After resampling the number of samples equals 5120 (T_{sym}=10T_s)

performed. Therefore only cycle frequencies related to the symbol rate must be taken into account in this cyclostationary analysis. Table 6.2 shows the cyclic frequencies $\alpha = T_{sym}$ for four different modulation types. The pulse shaping filter used before transmission results in a disappearance of cycle frequencies $\alpha = k/T_{sym}$ for $k > 1$. This is shown by Figure 6.9.

The CTCF can be completely evaluated for lag vector $\tau = [\tau_1 ... \tau_M]$, with order M. However, in [16] it was found out that complexity can be reduced by only evaluating the function for lag vector $\tau = [\tau_1, 0, .., 0]$. This can further reduced by evaluating τ_1 for a limited amount of lags. Later in this section, it will be explained why we should evaluate more τ values if the order increases. From Table 6.2 one can already conclude that the set (BPSK,PAM4) can be separated from (QAM16,QPSK) based on the location of it's cycle frequencies only based on the CTCF $C^{\alpha}_{yy^*}$.

However, the second and fourth order CTCF have the same cycle frequencies for both sets. Therefore we should go to higher orders and search for cycle frequencies that they don't have in common. It was found out that if we go to higher orders the peaks at the cycle frequencies become weaker. Figure 6.10a shows the cyclic autocorrelation function for τ_1 equal to zero, $\tau_2 = [-20 : 20]$ and $\alpha = [-0.2 : 0.2]$ for a BPSK modulated signal. At every τ-value the signal will have cyclostationary features at $\alpha = 1/T_{sym}$.

Theoretically, the function C_{yyyy^*} will have cyclic frequencies $\alpha = 1/T_{sym}$ at every value of τ_2. However, from Figure 6.10b it can be seen that for $\tau_1 = [-10 : 10]$ the peak at $\alpha = 1/T_{sym}$ becomes rather weak. It turned out that, especially for higher order cyclostationarity the α-peaks are getting weaker. It is also hard to predict, without the knowledge of the exact modulation type, at what lag parameters τ the cyclic frequency $\alpha = 1/T_{sym}$ will be high enough to see an actual peak value. Therefore, to find a peak value α in a higher order cyclostationary analysis, multiple values of τ must be evaluated requiring more operations. Figure 6.10c shows the CAF for a QPSK modulated signal evaluated for the same parameters as for Figure 6.10a. One can see the same result, meaning that both BPSK and QPSK have the same cyclostationary properties for $C^{\alpha}_{yy^*}$.

Referring to Figure 6.10d, where the function C_{yyyy^*} is evaluated for QPSK, there are no clear cycle frequencies α as a function of the symbol rate T_{sym}. This is according the presented cycle frequencies from Table 6.2.

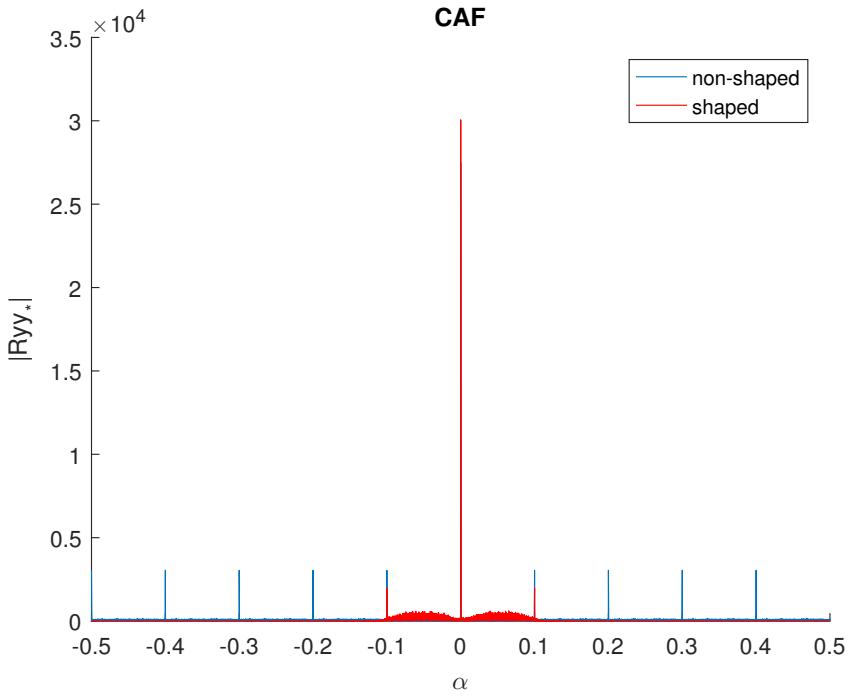

Figure 6.9: A pulse shaping filter before transmission results in the disappearance of peaks at cycle frequencies $\alpha = k/T_{sym}$ for $k > 1$.

	$C_{yy}^{\alpha} = R_{yy}^{\alpha}$	$C_{yy^*}^{\alpha} = R_{yy^*}^{\alpha}$	C_{yyyy}^{α}	$C_{yyyy^*}^{\alpha}$	$C_{yyy^*y^*}^{\alpha}$
BPSK	$[-T_{sym}, 0, T_{sym}]$	$[-T_{sym}, 0, T_{sym}]$	$[-T_{sym}, 0, T_{sym}]$	$[-T_{sym}, 0, T_{sym}]$	$[-T_{sym}, 0, T_{sym}]$
PAM4	$[-T_{sym}, 0, T_{sym}]$	$[-T_{sym}, 0, T_{sym}]$	$[-T_{sym}, 0, T_{sym}]$	$[-T_{sym}, 0, T_{sym}]$	$[-T_{sym}, 0, T_{sym}]$
QPSK	-	$[-T_{sym}, 0, T_{sym}]$	$[-T_{sym}, 0, T_{sym}]$	-	$[-T_{sym}, 0, T_{sym}]$
QAM16	-	$[-T_{sym}, 0, T_{sym}]$	$[-T_{sym}, 0, T_{sym}]$	-	$[-T_{sym}, 0, T_{sym}]$

Table 6.2: Theoretical cycle freqeuncies of four different modulation types. So evaluating C_{yy}^{α} for a BPSK modulated signal results in peak values at $-T_{sym}, 0, T_{sym}$.

6.3. Constant Envelope Modulation

In contrast to non-constant envelope modulated signals, constant envelope modulated signals can't be distinguished based on their constellation diagram. Therefore another approach is needed to resolve this problem. The signals that are analysed are from the set (M-FSK, GMSK, MSK). The main focus of this research project was on the non-constant envelope modulated signals. Some remarks on the identification of constant envelope modulated signals will be given.

6.3.1. Symbol Rate Estimation

To estimate the symbol rate of a signal from the set (M-FSK, GMSK and MSK) a approach is chosen that has some overlap with the approach of estimating the symbol rate for a non-constant envelope modulated signal. However instead of applying the algorithms on the amplitude or phase information, it is applied on the frequency information. This is done by doing the following operation on the received signal samples:

$$f[n] = \big(\phi[n] - \phi[n-1]\big)\frac{1}{2\pi T_s} \tag{6.12}$$

This frequency information can then be used to solve the following optimization problem:

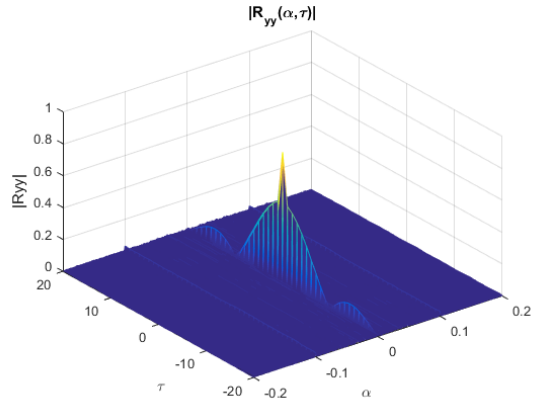

(a) SNR=5dB. The cyclic autocorrelation function R_{yy^*} evaluated for a BPSK signal

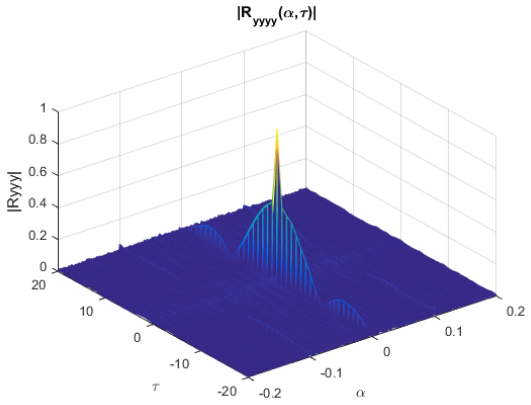

(b) SNR=5dB. The cyclic temporal moment function R_{yyyy^*} evaluated for a BPSK signal

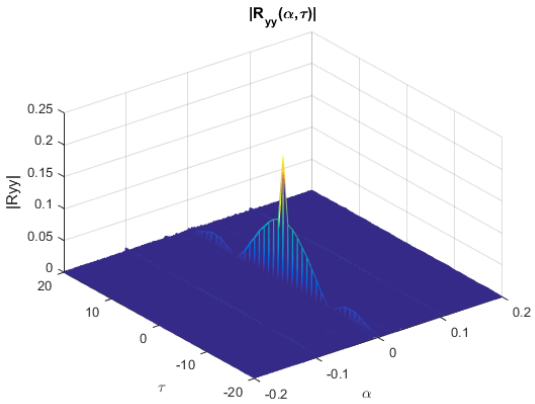

(c) SNR=5dB. The cyclic autocorrelation function R_{yy^*} evaluated for a QPSK signal

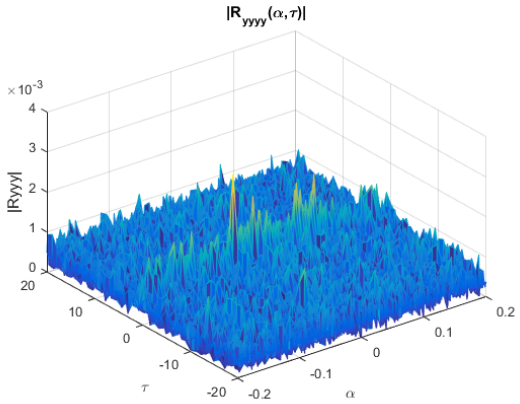

(d) SNR=5dB. The cyclic temporal moment function R_{yyyy^*} evaluated for a QPSK signal

Figure 6.10: Second and higher order cyclostationary analysis for two different modulation types.

$$\max_{\alpha_i \in W_f} \left| \sum_{n=0}^{N_T-1} |f[n]|^2 e^{-i2\pi\alpha_i n T_s} \right|, \tag{6.13}$$

Resulting in a cycle frequency at $\alpha = 1/T_{sym}$.

6.4. Resulting Decision Tree

A generalized framework was proposed to compare methods that can identify the modulation type, symbol rate and carrier offset. Within this framework, the best methods are found in terms of complexity and performance. This was done by looking at the unique characteristics of every modulation type. Furthermore, pre-processing is performed before the actual modulation classification to be able to use low complexity algorithms in later steps. For example, an ASK modulated does not have phase information, so a low complexity algorithm can be used to distinguish between ASK and non-ASK modulated signals. However, when an ASK signal is contaminated with a frequency offset it is indistinguishable from other linear modulation types based on the phase information. Therefore, this frequency offset is first calculated and removed. Then, a low complexity algorithm can be used to discriminate between ASK and non-ASK modulated signals. The relation between modulation classification performance, complexity and the required preprocessing is taken into consideration in every decision step. As explained in Chapter 4, two commonly used classifiers are the decision tree and pattern recognition. It was decided to use a decision tree classifier, since this is easier to expand with more modulation types. The power of the proposed generalized framework in Chapter 3 is that unknown modulations can easily be analysed within this framework. So after analysing an unknown modulation type within this framework, the decision tree can be expanded. The proposed decision tree, according to the algorithms presented in previous sections, is shown by Figure 6.11.

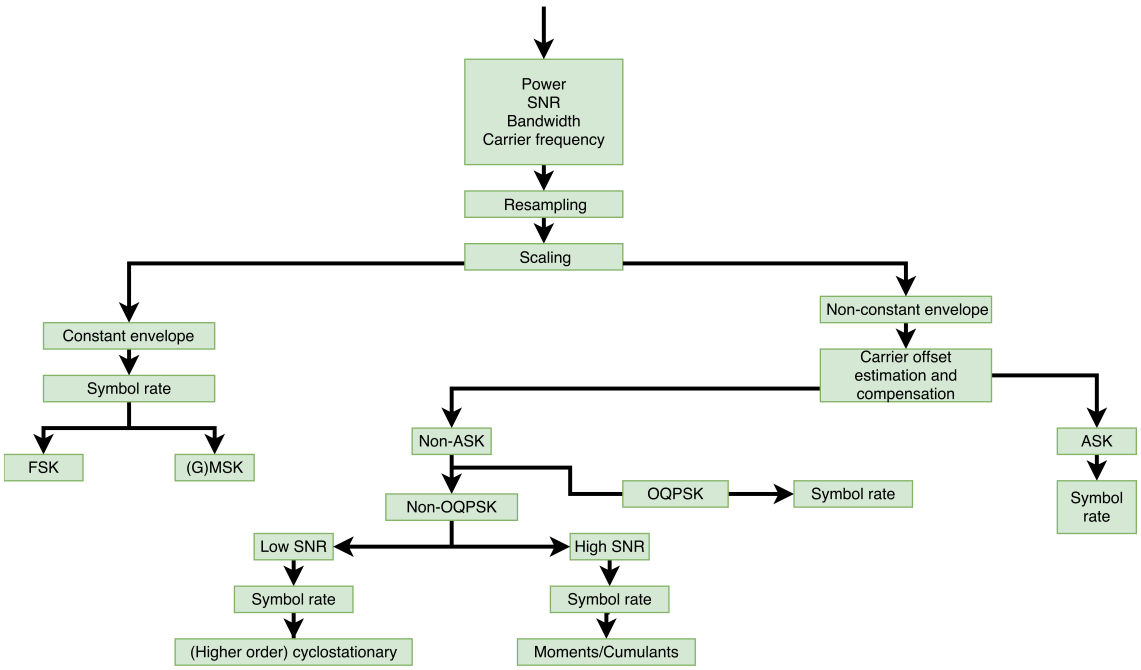

Figure 6.11: Block diagram of the proposed decision tree.

6.5. Performance of the Decision Tree

This section will first show the performance of this decision tree for different modulation types. It turned out that even at low SNR (SNR>5dB) that the discrimination between constant envelope modulation (M-FSK, (G)MSK) and non-constant envelope modulations (M-PSK,M-QAM,M-PAM, M-ASK) can reliably made if we adaptively change the threshold as a function of SNR. No preprocessing is needed (except for resampling and amplitude scaling) to make this decision.

The carrier offset can than be estimated for all modulation types from the set (M-PSK,M-QAM,M-PAM, M-ASK). Figure 6.12 shows the classification performance of 6 different modulation types as a function of the signal to noise ratio. The frequency offset was randomly generated between 0.001 and 0.00001 f_o/f_s. So the frequency offset f_o is relative to the sampling frequency f_s. The phase offset Φ_{ch} was randomly generated between 0 and 360. The modulation type from the chosen set (ASK2,BPSK,OQPSK,PAM4,QAM16,QPSK) was randomly generated 1000 times at every SNR. The number of bits before modulation was 5120. Those bits where then mapped on a symbol sequence. QAM16 has 4 bits per symbol whereas BPSK has 1 bit per symbol. So depending on the modulation type, we have different number of symbols. Then, together with the pulse shaping filter, the signal was upsampled with a factor 10. This means that the simulated BPSK has $5120/1 * 10 = 51200$ symbols whereas QAM16 has $5120/4 * 10 = 13025$ symbols. Now this data, with a random phase and frequency offset, is tested for different SNR's. The threshold for the last decision step was according to:

$$\text{BPSK:} \quad C_{42} < -1.5 \tag{6.14}$$

$$\text{PAM4:} \quad -1.5 < C_{42} < -1.1 \tag{6.15}$$

$$\text{QPSK:} \quad -1.1 < C_{42} < -0.75 \tag{6.16}$$

$$\text{QAM16:} \quad -0.75 < C_{42} < -0.4 \tag{6.17}$$

$$\text{None:} \quad C_{42} > -0.4 \tag{6.18}$$

These thresholds were set based on the theoretical values of the cumulant C_{42} which are given in subsection 6.2.5. Referring to Figure 6.12 one can see that a reliable decision can be made if the SNR>18dB. For ASK2 the right decision can be made even if the SNR is as low as 5dB. Since at that point the frequency offset is removed we can use a low complexity algorithm that uses the absence of phase information in the signal.

Looking at the classification performance of an OQPSK signal, one can bee that we can reliably classify it at an SNR>8dB. This is remarkable because it has the same constellation diagram as normal QPSK. However, referring back to subsection 6.2.3 we use a cyclostatonary analysis to classify it as a OQPSK signal. It is important to make the decision for OQPSK or a non-OQPSK signal, because the symbol rate can't be found in the same way. Since cyclostaionary methods can work at low SNR-regions this method works at low SNR.

The classification of the signals from the set (BPSK,PAM4,QAM16,QPSK) is done based on the distribution of the IQ points in the constellation diagram. From Figure 6.12 it looks if the modulation type QAM16 is correctly classified at an SNR>7. However, the cumulant value C_{42} for all modulation types converges to zero if the SNR goes to zero (see previous chapter). Because QAM16 is correctly classified if $-0.75 < C_{42} < -0.4$ all modulation type will be in this range if the SNR will get lower. So at low SNR, all modulation types will be misclassified as QAM16. This can't be solved by using a stationary method (moment, cumulant).

6.6. Stationary and Cyclostationary Classification

The point where we use the cyclostationary properties of an unknown signal is when we are in a low SNR reqion. From Figure 6.12 it can be seen that for the chosen method, the threshold lies around 18dB. Based on second order cyclostationarity, one can already distinguish between the set (BPSK,PAM4) and (QPSK,QAM16). In other words a discrimination can be made between modulation types that only have real valued constellations and modulation that are have both real and complex valued constellations. This is showed by a comparison between a stationary cumulant method and a cyclostationary method. We know that QPSK/QAM has no conjugate cycle frequencies R^{α}_{yy} and non-conjugate cycle frequencies $R^{\alpha}_{yy^*}$ at $[-1/T_{sym}, 0, 1/T_{sym}]$. In contrast, PAM/BPSK have cycle frequencies at $[-1/T_{sym}\ 0\ 1/T_{sym}]$ for both the conjugate and non-conjugate case. Therefore a four dimensional feature vector was made:

$$F = [R^0_{yy^*}, R^{-\alpha}_{yy}, R^0_{yy}, R^{\alpha}_{yy}] \tag{6.19}$$

$$F_{QPSK} = [1,0,0,0] \tag{6.20}$$

$$F_{PAM} = [1,1,1,1] \tag{6.21}$$

This feature vector F is calculated from the received waveform, where only PAM4 and QPSK are taken into consideration. The resulting feature vector is then compared in the least squares sense with the theoretical

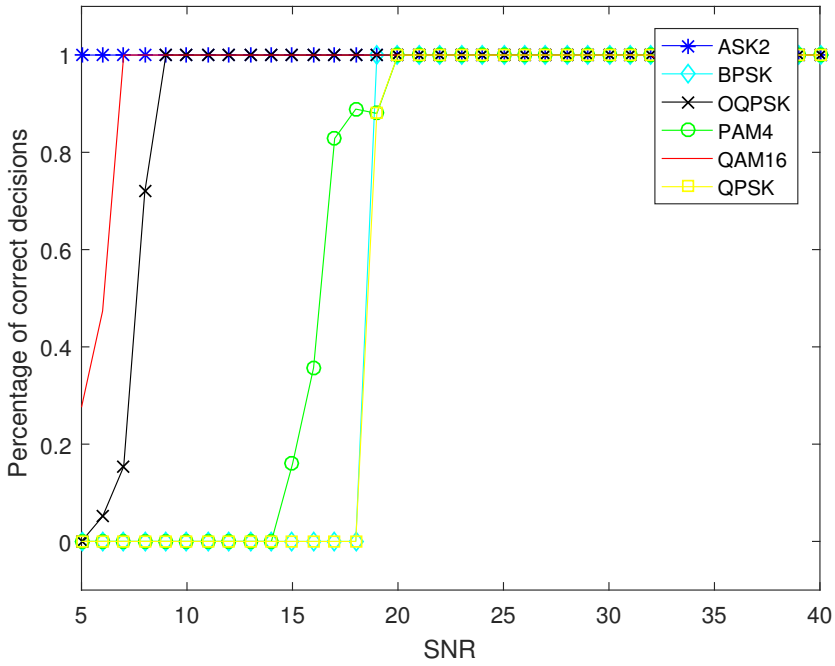

Figure 6.12: Probabilty of correct classification for six different modulation techniques as a function of the SNR (in dB).

feature vectors from PAM4 and QPSK. A low value in the least squares sense means that the calculated feature vector matches the theoretical value. Figure 6.13 shows the least squares value of a simulated QPSK signal for different SNR's. This figure is obtained by simulating a QPSK 100 times at every SNR for a random phase and frequency offset.

It can be seen that form a SNR>8 the signal can be reliably classified because the least squares value for theoretical QPSK lies below the least squares value of theoretical PAM4 .
To show the added value of cyclostationary analysis of a low SNR signal, the stationary en cyclostationary methods are compared. The thresholds from Equation 6.14 are rewritten because a 4-class problem is reduced to a 2-class problem. So instead of discriminating between four modulation types (QPSK,QAM16,BPSK,PAM4) we will now discriminate between two modulation classes (BPSK,PAM) and (QAM16,QPSK). So a four class problem reduces to a two class problem. The threshold is set according to:

$$\text{BPSK,PAM4:} \quad C_{42} < -1.1 \tag{6.22}$$

$$\text{QAM16,QPSK:} \quad -1.1 < C_{42} < -0.4 \tag{6.23}$$

$$\text{None:} \quad C_{42} > -0.4 \tag{6.24}$$

These thresholds were set based on the theoretical values of cumulant value C_{42}. This stationary method is now compared with the cyclostationary method. Again the frequency and phase offset are randomly generated. QPSK, QAM16,PAM4 and BPSK are randomly generated 50 times at every SNR. Figure 6.14 shows the performance of both the stationary en cyclostationary method. It shows that using a cyclostationary method will make (mostly) a correct classification for an SNR>10dB whereas a stationary method will do this for only SNR>19dB.

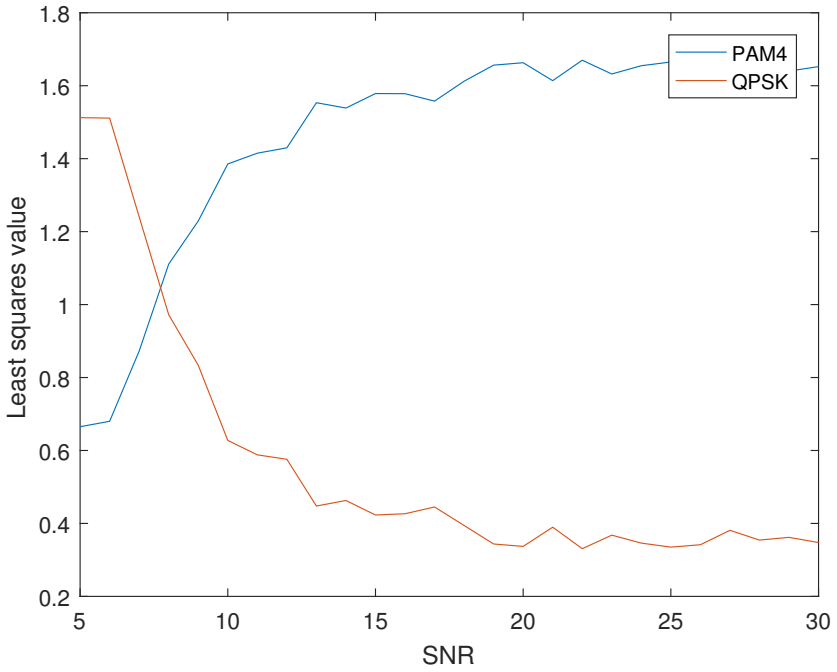

Figure 6.13: Least squares value for a calculated feature vector of a QPSK signal compared with the theoretical feature vectors of QPSK and PAM as a function of the SNR (in dB).

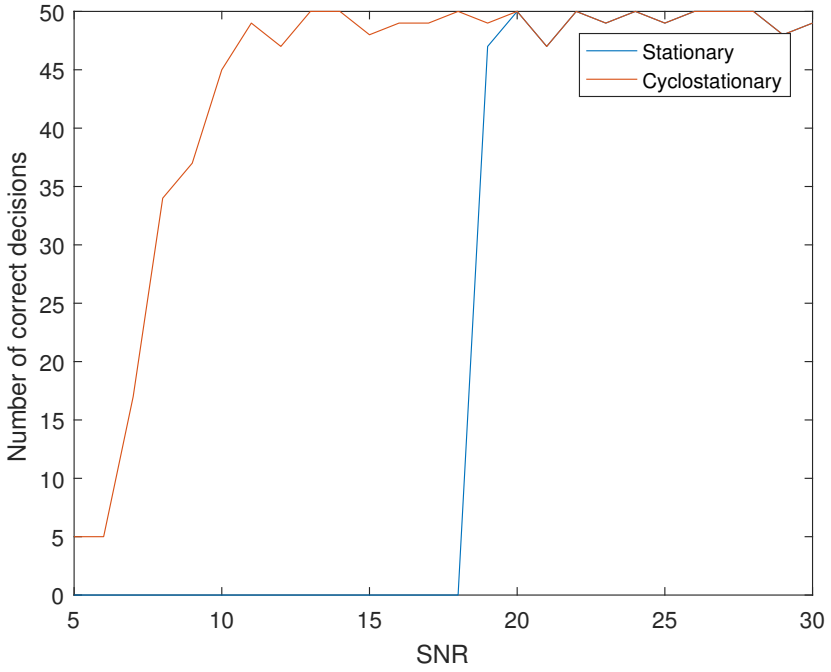

Figure 6.14: Comparison between stationary and cyclostationary modulation classification

7

Conclusion and Discussion

In the introduction the problem statement was defined:

Can we extract the symbol rate, carrier offset and modulation format from raw IQ-data when coarse estimates of the bandwidth, center frequency, SNR and burst length under signal contamination are available while also minimizing computational complexity?

Blind signal identification was first placed in a military context. It was described why signal identification is important in this context. A SDR platform is the basic platform where the identification process is performed and the use of a SDR directly gives some implications that we can make use of. This is because the SDR front-end already performs some processing. Complete blind identification will therefore reduce to a more semi blind identification where there is a coarse estimate of some parameters. Those parameters are the SNR, carrier frequency, power, bandwidth and continuous/burst. Having a coarse estimate of those parameters allows for the use of less complex algorithms.

By first presenting a general signal model, the methods can be evaluated within this model. The signal model also demonstrates what type of signal contamination we have to deal with. The sum of the contamnination sources can be reduced to a timing offset, phase offset, frequency offset and unknown uncorrelated noise. It further describes the properties of a communication signal and what uniquely defines it. Emphasis was put on the a pulse shaping filter because it has important implications in the modulation classification process.

A literature study was performed on the topic of blind signal identification with the main focus on digital single carrier modulated signals. Especially automatic modulation classification is a broad research area. There is however no silver bullet i.e. a method that can classify all modulation types. Most methods solve just a subset of the problem meaning that a limited amount of modulation types can be classified within limited amount of signal contamination. Therefore, comparing methods is an infeasible task. To deal with this problem the unique characteristics of a communication signal are identified.

A framework is built based on LOS, HOS, SOCS and HOCS. Describing a signal in the LOS and HOS framework are stationary methods whereas describing a signal in the SOCS and HOCS are cyclostionary methods. This makes it easier to compare classification methods in terms of performance and complexity. It also has the advantage, that if an unknown modulation comes into play, we can analyse this within this framework. Digital single carrier modulated communication signals can transfer information by periodic keying of amplitude, phase and/or frequency (or a combination of these). This periodicity in the statistics of a communication signal can be modelled as cyclostationary. To completely characterize a signal as cyclostationary, is computationally a demanding task. If we go to higher order cyclostationarity the complexity grows exponentially if the complete function is evaluated. Therefore, there is a search for algorithms that can classify modulation types with less computations. The theory of moments and cumulants is adopted which can actually be viewed as a subset of the cyclostationary feature space.

The key is to identify the unique characteristics of the unknown signal and find the least complex solution within this framework. In general, low complex stationary methods need preprocessing before the actual modulation classification can be done. A good example is the classification of ASK and non-ASK modulated signals. It is known that ASK modulation does not have phase information meaning that the phase is constant. However, when ASK is transmitted over a channel and mixed down to baseband it will have some frequency offset. This offset results in changing phase value as a function of this offset. By first removing this frequency offset, a low complexity algorithms can then be used that is within the LOS framework: the standard deviation of the instantaneous phase.

Based on the knowledge of single carrier digital modulated signals and the classification complexity within this framework, a decision tree was built. This decision tree has the ability to reliably classify signals from the set (BPSK, M-PSK, M-QAM, M-ASK, M-PAM and OQPSK) when the SNR matches certain criteria and allows for intuitive extension to other modulation types. Furthermore, it was found out that signals that have similar characteristics (QPSK and QAM16) can be distinguished based on the constellation diagram if the SNR is high enough and preprocessing is performed. Those algorithms are based on moments and cumulants from the LOS or HOS framework. If we are operating in a low SNR region, single carrier digital modulation types can still be distinguished. However, more computationally demanding algorithms are needed from the SOCS and HOCS framework. Those cyclostationary methods were tested to make a separation between signals from the set (QPSK, QAM) and (BPSK,PAM4). A cyclostationary analysis can make this separation even when the SNR is just 8dB. Within this decision tree, also the symbol rate and the carrier offset must be found. Both methods are a subset of the cyclostationary feature space, meaning that not the complete cyclostationary statistics must be evaluated but just a smart subset. The determination of the symbol rate and carrier offset are placed in the decision tree in a smart way so that this information can be reused in later steps. The emphasis of this research project was on the linear single carrier modulated communication signals. However, by using the developed knowledge and framework, also the non-linear modulations are analysed. This can be done by looking at the frequency content of the received waveform instead of the phase and amplitude content.

A literature study showed that cyclostationary signal processing has applications in modulation classification but also in symbol rate and carrier offset estimation. A lot of effort was put in understanding the theory behind cyclostationarity and how it can be used in this military context. It showed less potential then expected, because low complexity stationary methods turn out to have similar performance in terms of modulation classification in a lot of cases especially when preprocessing on the data is applied. Even in low SNR regions, where cyclostationary signal processing perform better, the results are hard to interpret without any prior knowledge. Generally, if the complete cyclic autocorrelation or spectral correlation is blindly calculated from the received signal without any preprocessing, the modulation type can't be immediately classified. A directed search for cycle frequencies is needed by first subdividing modulation types into classes. This was showed by first subdividing constant envelope and non-constant envelope modulated signals with a low complexity algorithms. Within the subgroup of non constant envelope we can then further subdivide into ASK and non-ASK modulated signals by a low complexity algorithms. The remaining (non-ASK modulated) signals can then be classified by searching for specific cycle frequencies that uniquely defines them.

8

Future Work

The algorithms that are developed were based on simulated data making it possible to generate signals with desired parameters. In a practical implementation, more (unknown) signal contamination is possible. Therefore the algorithms must be robust in these circumstances. Especially when parameters or signal contamination change over time. In a simulation environment, more samples will give a more reliable estimate of signal statistics. But when the signal contamination changes over time it could be beneficial to analyse smaller sample sets, making the chance higher for constant statistics within each sample set. This gives a trade-off between the number of samples (complexity) and classification performance. Especially in the stationary framework, it could be beneficial to calculate the statistics in a sliding window approach. So the sample set will be subdivided into smaller overlapping segments and averaged over the number of segments.

The modulation types that were taken into account are just a subset of all possible modulation types. Naturally, the decision tree could be expanded with single carrier analogue modulations. Nowadays, most signals in the electromagnetic spectrum are digital signals and, therefore, fit in the cyclostationary framework, but also analogue signals are present. Those signals do not fit in the cyclostationary framework since it lacks cyclostationary behaviour because of the absence of periodic keying in either the phase, amplitude or frequency. A search must be done for algorithms that can distinguish between analogue and digital modulation techniques in an early stadium of the decision tree.

The use of higher order cyclostationary as a modulation classifier was explained in the previous chapters. It was shown that the complete evaluation of a signal as higher order cyclostationary requires a lot of computations. The number of computations can be reduced by evaluating the function for subset of the lag parameter $\tau = [\tau_1, .., \tau_M]$ with M the order. In a blind scenario, it is hard to predict for which values of τ the CTCF must be evaluated to have the best classification performance. Furthermore, the cyclostationary properties are only evaluated up to order 4 in this research project. Going to higher orders will theoretically result in the possibility of the classification of signals that have similar second and fourth order characteristics (QPSK and QAM16).

In a military context, the most interesting signals in the electromagnetic spectrum could be short burst transmissions. From an opponent point of view, the interception probability will decrease. If a bursty transmission is picked up by a SDR, the number of available samples is limited. This implies that a search must be done on the minimum amount of samples needed to reliably identity this unknown burst transmission.

A

QPSK modeling

According to the definitions of Chapter 2 a received single carrier modulated signal, that is mixed down to baseband and digitized, can be mathematically described as:

$$y[n] = \epsilon_A e^{-i\Phi_{ch}} * e^{-i2\pi f_o n T_s} \sum_l g[n - l T_{sym}/T_s] A[l] e^{-i\phi[l]} + v[n] \tag{A.1}$$

with amplitude $A(l)$, gain factor ϵ_A, frequency offset f_o, symbol rate T_{sym}, T_s the sampling rate of the receiving device (so oversampled by $P = T_{sym}/T_s$, $\phi[l]$ the phase of the original waveform, Φ_{ch} the phase offset due to the channel, transmit filter g and $v[n]$ uncorrelated noise. This definition of a single carrier digital modulated signal will now be applied to QPSK modulated signal.

A.1. Ideal Case

First, the most simple form will be shown, where the influence of the channel will be ignored and no shaping filter is used before transmission. The received digitized waveform, after perfect down mixing to baseband, is described as:

$$y[n] = A[n] e^{-i\phi[n]} \tag{A.2}$$

where the pair (A, ϕ) must be from the set $[(1,0)(1,\pi/2)(1,\pi)(1,3\pi/2)]$. This results in the waveform and constellation plot from Figure A.1 showing the 4 discrete states. Since no pulse shaping filter is used the transitions between states will be instantaneous. In practise, this will not be realizable.

A.2. Frequency Offset

When a frequency offset f_o is applied the equation is as follows (again with the same (A, ϕ)) pair:

$$y[n] = A[n] e^{-i(2\pi f_o n T_s + \phi[n])} \tag{A.3}$$

In this model we assume that the frequency offset is constant over time. In most real communication systems this does not hold. This means that the frequency offset must be tracked and compensated accordingly. For now this variation in frequency offset will be neglected. The constellation plot is shown by Figure A.2. A positive valued frequency offset will result in a clockwise rotation of the constellation plot whereas a negative valued offset results in a counter clockwise rotation.

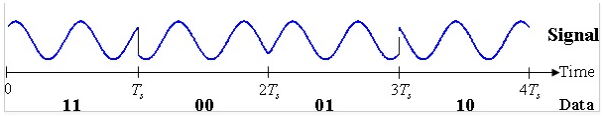

(a) Time domain

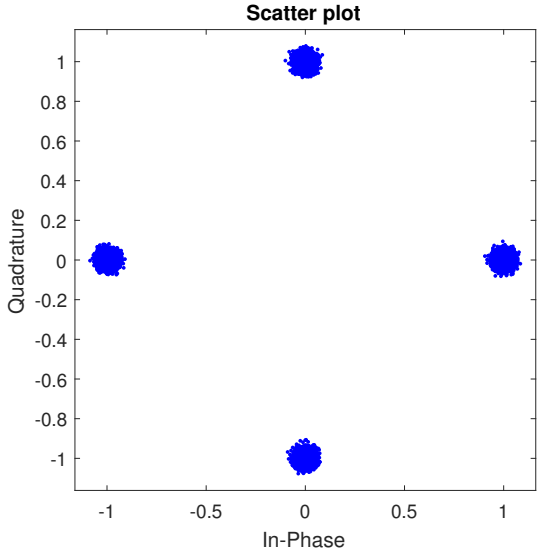

(b) Scatter plot

Figure A.1: (a) Time domain representation of QPSK where the bits are mapped on a waveform. Every time step T_s the symbol is changed meaning that T_s/T_{sym}=1. (b) Constellation plot of QPSK, where the in-phase represents the real part of the data and the quadrature the imaginary part of the data.

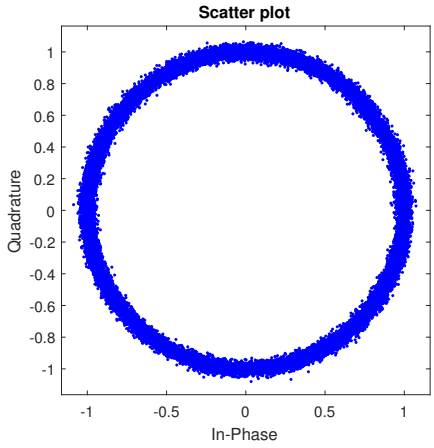

Figure A.2: The freqeuncy offset is given by $f_o = f/f_s = 0.001$, where the offset f_o is relative to the sample frequency f_s.

A.3. Phase offset

If there is a phase offset (Φ_{ch}) due to the channel can be modelled as:

$$y[n] = A[n]e^{-i(\phi[n]+\Phi_{ch})} \tag{A.4}$$

The same assumption from previous section holds for phase noise: It's assumed to be constant over the sample set. The constellation plot is given by Figure A.3.

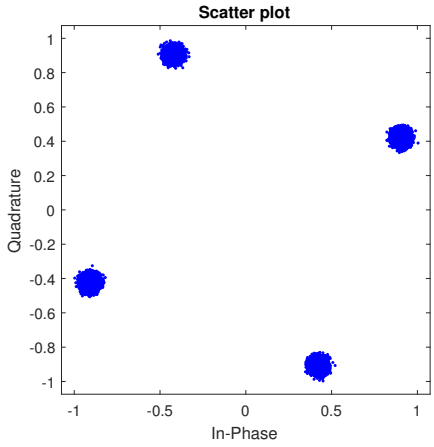

Figure A.3: QPSK signals with a phase offset equal to 25 deg. This phase offset is assumed to be constant over the sample set.

A.4. Pulse Shaping

Another important parameter that influences the waveform is the use of a pulse shaping filter. In real world systems, communication signals must me band-limited to prevent interference and overlapping spectra. Therefore, a shaping filter will always be present. Analysing the influence of a shaping filter on the identification performance is very important for that reason. The received waveform with the use of a shaping filter, can be described as:

$$y[n] = \sum_l g[n - lT_{sym}/T_s]A[l]e^{-i\phi[l]}, \tag{A.5}$$

where g is a root raised cosine filter with $0 < \beta < 1$ and l is the filter length. The resulting constellation diagram is now given by Figure A.4. As can be seen from this figure there are not only discrete states but also

data points in between. This means that it will be difficult to distinguish between modulation types based on this constellation diagram when shaping is applied to the transmitted signal. However if we have knowledge about the signals symbol rate it can be re-sampled accordingly. Ideally we would have knowledge about the used pulse shaping filter because then at the receiving side a matched filter can be applied.

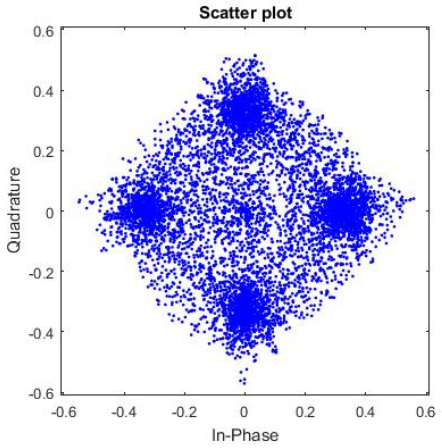

Figure A.4: QPSK signal where a root raised cosine filter is used. It's parame

A.5. Timing Offset

An optimal receiver will have an sample clock that is aligned with the transmitter. Sampling the received waveform at the optimal point will result in the highest possibly of correct decision of which symbol was transmitted. In blind signal identification, the symbol time of the transmitted waveform is not known a priori. Another parameter which is not really flexible is the sampling frequency of the receiving SDR because this depends on the device. Therefore the compensation for a timing offset can only be done in software. If we are able to find the symbol rate T_{sym} the original signal can be resampled at it's optimum sample points.

A.6. Added Noise

Noise is another parameter that influences the performance of a communication link. For simplicity, noise is modelled as additive white Gaussian noise process. It has the property of having equal power in every frequency band. Furthermore, in the time domain it is normal distributed with a zero average. If this noise is added to a QPSK signal the equation will be as follows:

$$y[n] = A[n]e^{-i\phi[n]} + v[n] \tag{A.6}$$

Figure A.5 shows the constellation diagram for different SNR's. Looking at those constellation diagrams, the SNR lower limit where QPSK can be correly classified is somewhere around 5dB by visual inspection. Later on in this appendix it will be explained how this visual interpretation can be translated to statistical descriptions.

A.7. Attenuation

Propagation of a communication signal will inherently result in attenuation. this can be modelled by:

$$y[n] = \epsilon_A A[n]e^{-i\phi[n]} \tag{A.7}$$

For blind signal identification the exact knowledge of the attenuation between transmitter and receiver is not really important. We just want to receive a unknown signal with high enough SNR and not what the original power was at the transmitting side. However, the gain factor ϵ_A must be compensated so it has unit energy before the identification algorithms. This will prevent scaling problems in later steps.

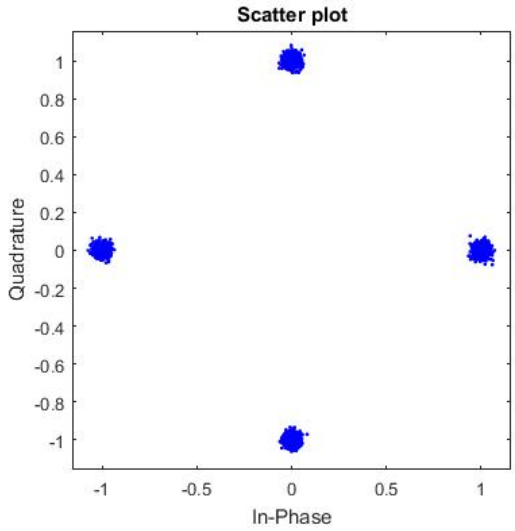

(a) SNR=30dB

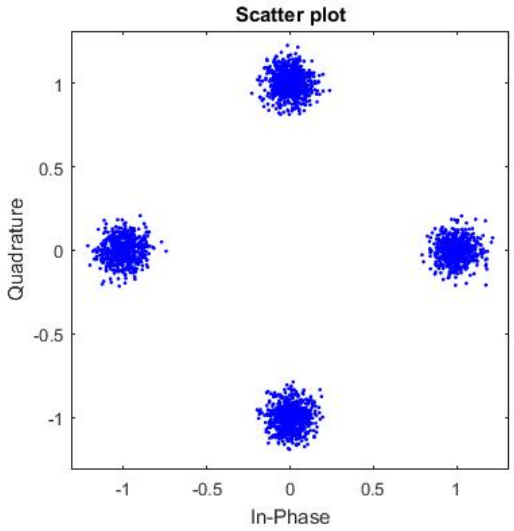

(b) SNR=20dB

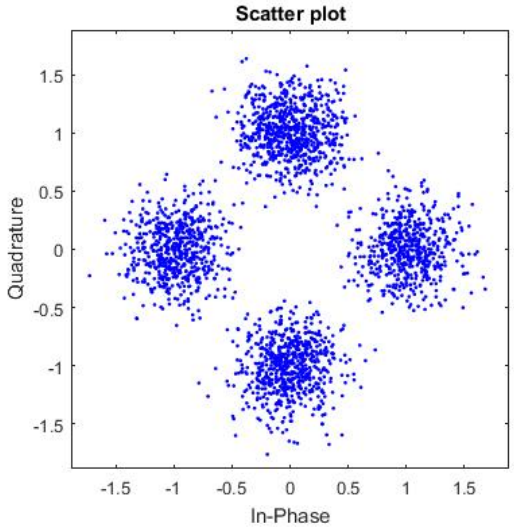

(c) SNR=10dB

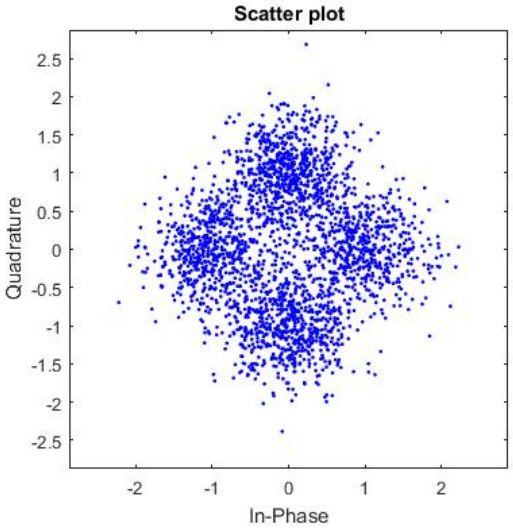

(d) SNR=5dB

Figure A.5: Constellation plot of a QPSK modulated signal for different Signal to Noise Ratios

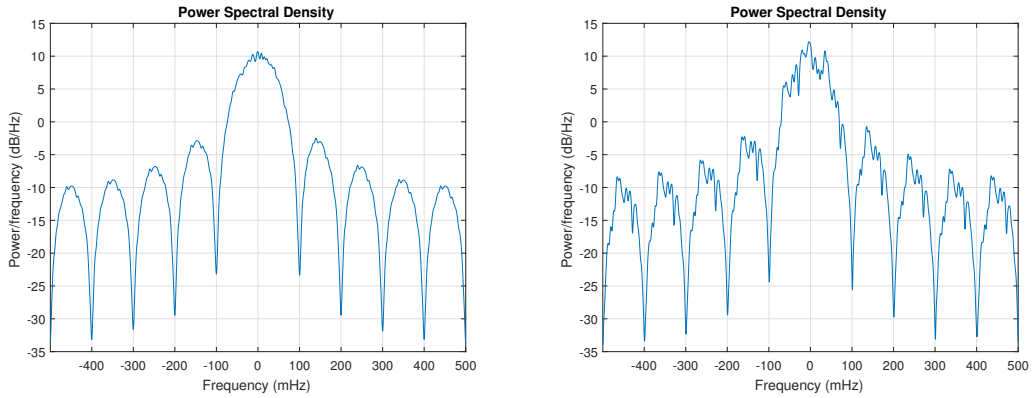

(a) PSD with overlapping Welch window

(b) PSD without overlapping

Figure A.6: Comparison between the PSD's of a QPSK signal where different parameters are chosen for the PSD calculation

A.8. Identification Algorithms

Now we have described all the aspects of the channel that we take into account, we can show their influence on the identification algorithms. Again, QPSK will be used to demonstrate their working principle. The next subsection will highlight the most important identification algorithms which are used in this thesis project.

A.8.1. Bandwidth Estimation

An important parameter of a unidentified communication signal is the bandwidth. Figure A.6a shows the power spectral density of a QPSK signal without any influence of the channel. It was obtained for a QPSK signal of length N=5210 and a 50% overlapping Welch window of length 256. Figure A.6b shows the same QPSK, but with different paramaters for obtaining the PSD. It was calcaulated by a PSD calculation for the complete length N of the sample set without overlapping windows. It can be seen that a different PSD is found by choosing the parameters differently. If our definition (-3dB point) of bandwidth is used on both PSD's slightly different values will be found. This example can be shown in a more extreme case resulting in a bigger discrepancy in bandwidth estimation for the same signal. From here it can be concluded that the bandwidth of an unknown signal can't be found exactly. However, in later steps only a coarse estimate of the bandwidth information is used as indication of the symbol rate making a coarse estimate sufficient.

A.8.2. Symbol Rate

The symbol rate of a digital single carrier modulated signal can be found by searching for cycle frequency $\alpha = 1/T_{sym}$ in the cyclic autocorrelation function. The definition of this CAF is given in chapter 3. If we apply the definition on the received complex samples $y[n]$ we will get:

$$R^{\alpha}_{yy^*}[n,\tau] = |\sum_n y[n-\tau]y^*[n] * e^{(-i2\pi\alpha nT_s)}| \tag{A.8}$$

$$= |\sum_n A[n-\tau]A[n]e^{(-i2\pi f_0 T_s((n-\tau)-n))} * e^{(-i2\pi\alpha nT_s)}| \tag{A.9}$$

$$= |\sum_n A[n-\tau]A[n]e^{(+i2\pi f_0 T_s\tau)} * e^{(-i2\pi\alpha nT_s)}| \tag{A.10}$$

$$= |e^{(+i2\pi f_0 T_s\tau)}|\sum_n A[n-\tau]A[n] * e^{(-i2\pi\alpha nT_s)}| \tag{A.11}$$

$$= |\sum_n A[n-\tau]A[n] * e^{(-i2\pi\alpha nT_s)}|, \quad \text{iff} \quad \Im(f_0\tau) = 0 \tag{A.12}$$

The condition $\Im(f_o\tau) = 0$ holds since both τ and f_o are real valued. Therefore the term $|e^{(+i2\pi f_0 T_s\tau)}|$ will not influence the amplitude in this CAF because it's amplitude always equals one meaning that the CAC function is not influenced by a phase or frequency offset.Figure A.7 shows this CAC function for a rectangular pulse shaped QPSK modulated signal. From this figure it can be seen that the chosen lag parameter τ is crucial for the determination of the cycle frequency $\alpha = k/T_{sym}$, where k is an integer value. For $\tau = 0$ the only peak

value is at $\alpha = 0$ but for $\tau = 1$ peak values appear at $\alpha = k/T_{sym}$. What also can be seen from Figure A.7 is that evaluating the CAF for lag parameter $\tau > 10$ will not result in a cycle frequency as a function of the symbol rate. This maximum value of the lag parameter is not random but related to the symbol rate which is $T_{sym} = 10$.

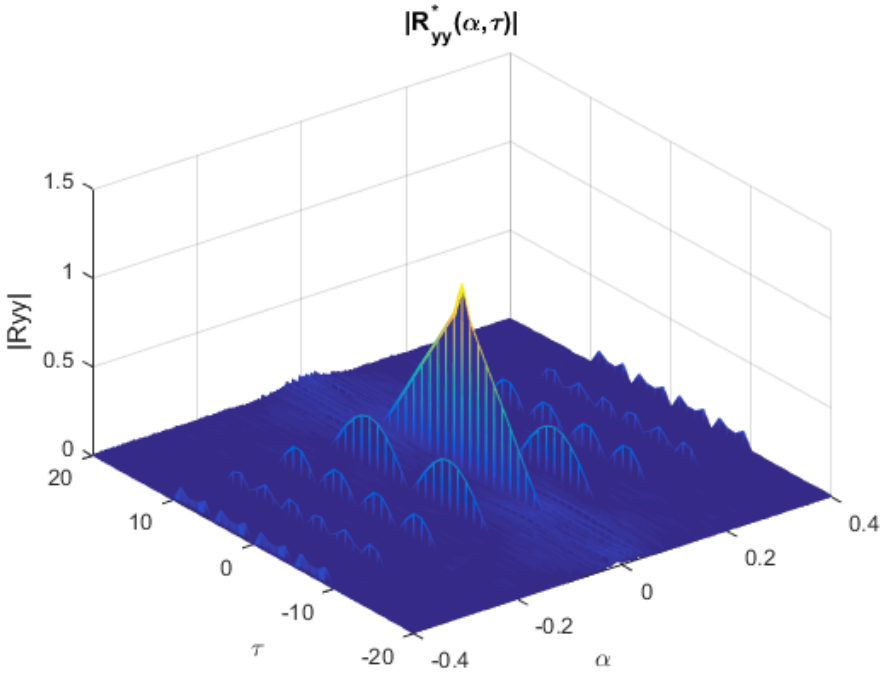

Figure A.7: Cyclic Autocorrelation function for a QPSK modulated signal.

We know that in practical systems a pulse shaping is used before transmission. Applying a root raised cosine filter, with $\beta = 0.2$ and filter length $l = 10$ results in a different CAF. This is shown by Figure A.8. The root raised cosine filter does not only change the spectral shape in the frequency domain. It also significantly changes the CAF in suppressing the amplitude of the cyclic peaks. The extreme case is when the roll-off factor of the root raised cosine filter equals 0. This results in complete suppression of the peaks at cycle frequency $\alpha = 1/T_{sym}$. In practise this is not realizable, because the filter needs to be infinitely long. So the cycle frequency at $1/T_{sym}$ will be suppressed whereas al other cycle frequencies at k/T_{sym}, with $k = 2,3,..$ will be completely removed. The CAF for the lag parameter $\tau = 0$ is given by Figure A.9 where we see a clear peak at cycle frequency $\alpha = 1/T_{sym}$.

A.8.3. Carrier Offset

The carrier offset of a QPSK signal can be found calculating the FFT of the fourth power of the received waveform. Then, finding the peak value at cycle frequency $\alpha = 4f_0$ returns this offset. This can be mathematically described as:

$$R^{\alpha}_{yyyy}[n,\tau = \mathbf{0}] = \sum_n y^4[n] * e^{(-i2\pi\alpha nT_s)} \tag{A.13}$$

$$= \sum_n A^4[n] * (e^{(-i2\pi f_o nT_s + \phi[n])})^4 e^{(-i2\pi\alpha nT_s)} \tag{A.14}$$

The pair (A,ϕ) was originally from the set $[(1,0)(1,\pi/2)(1,\pi)(1,3\pi/2)]$. Due to the fourth order order operation this set transforms to $[(1,0)(1,2\pi)(1,4\pi)(1,6\pi)]$. So the phase information is removed meaning that Equation A.13 reduces to:

$$R^{\alpha}_{yyyy}[n,\tau = \mathbf{0}] = \sum_n A^4[n] * (e^{(-i2\pi f_o nT_s)})^4 e^{(-i2\pi\alpha nT_s)} \tag{A.15}$$

This leads to a cycle frequency at $\alpha = 4f_c$. Applying the same theory from the previous section, one can see that a phase offset will not influence the carrier offset estimation performance.

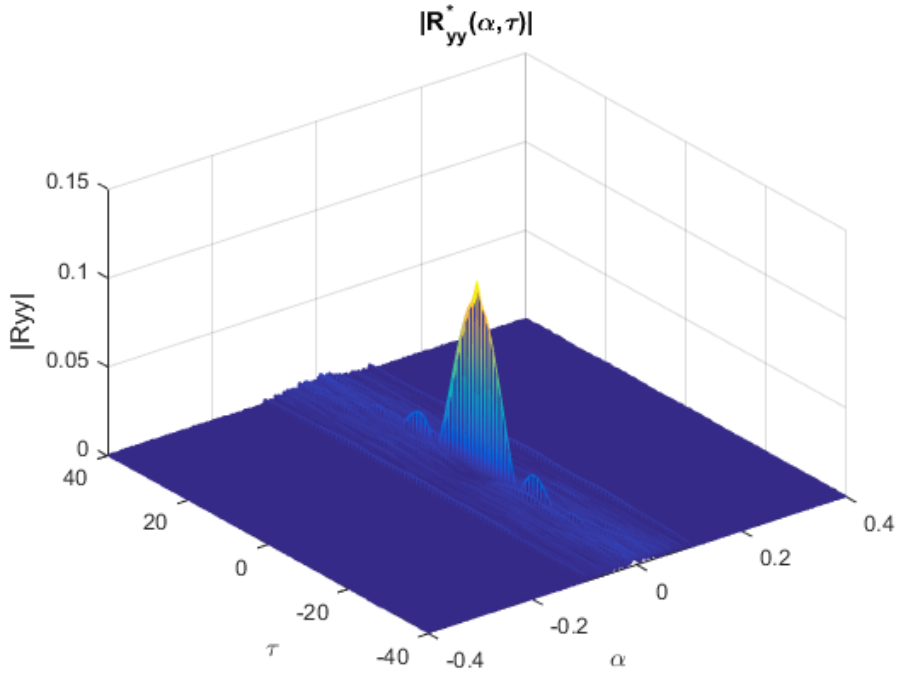

Figure A.8: Cyclic Autocorrelation function for a QPSK modulated signal where a root raised cosine filter is used as the transmit filter.

A.8.4. Moments and Cumulants

In chapter 3 a framework was proposed to statistically describe a communication signal. In this appendix it will be showed how this framework relates to this QPSK signal. The first order moment, estimated from discrete data is given by:

$$\hat{M}_1[n,\tau=0] = R_y^0[n,\tau=0] = \frac{1}{N}\sum_{n=0}^{N-1} y[n] \tag{A.16}$$

$$= \frac{1}{N}\sum_{n=0}^{N-1} A[n]e^{-j\phi[n]} = 0 \tag{A.17}$$

This shown by Figure A.10, where there red circle represents the mean value.
The second order centred moment from sampled data is given by:

$$\hat{M}_{21}[n,\tau=0] = R_{yy^*}^0[n,\tau=0] = \frac{1}{N}\sum_{n=0}^{N-1} y[n1]\,y^*[n] \tag{A.18}$$

$$= 1 \tag{A.19}$$

This is shown by Figure A.11, where again represents the mean value.
Both Equation A.16 and Equation A.18 are within the LOS framework. Furthermore, Equation A.18 can be seen as a subset of the cyclostationary statistics of a QPSK signal since it is evaluated for $\tau = 0$ and $\alpha = 0$.

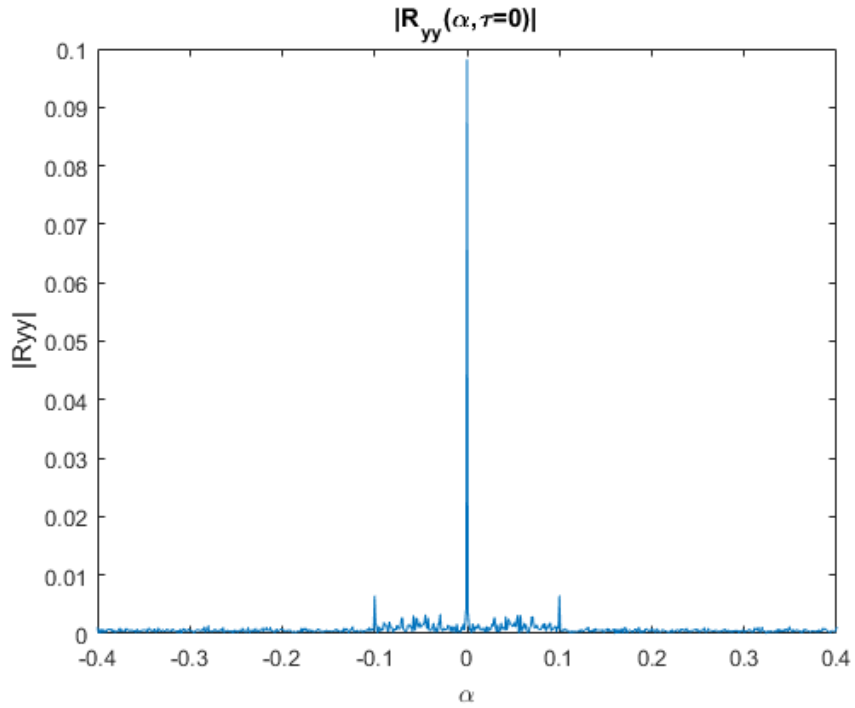

Figure A.9: Cyclic Autocorrelation function for a QPSK modulated signal where a root raised cosine filter is used as the transmit filter. This function is now evaluated for lag parameter $\tau = 0$

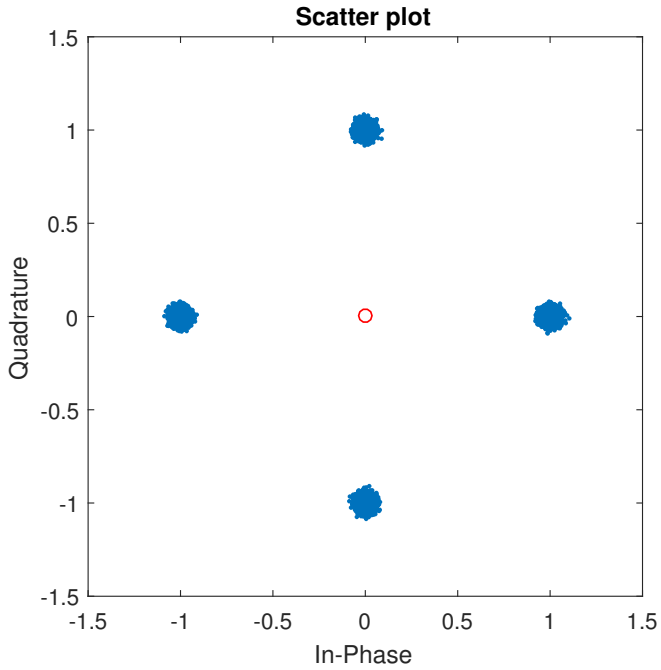

Figure A.10: Scatter plot of a QPSK signal where the red circle represents the average value.

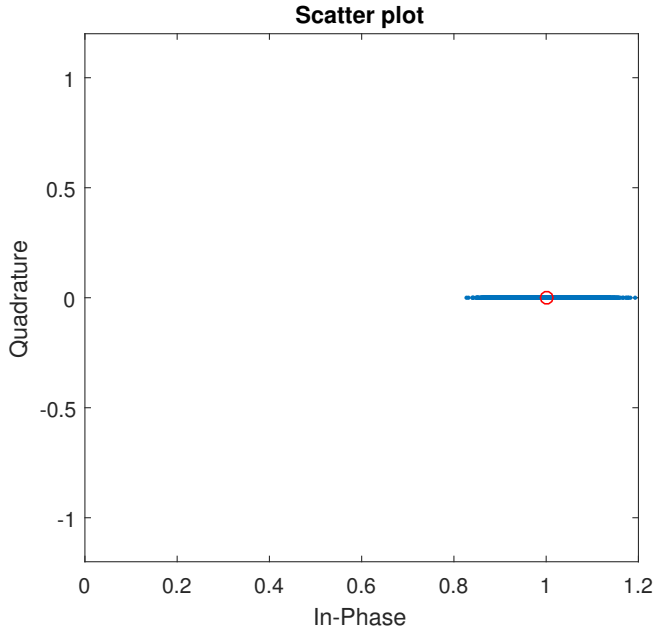

Figure A.11: Scatter plot of $y[n] * y[n]^*$ of a QPSK signal where the red circle represents the average value.

Bibliography

[1] Raised cosine filter. https://en.wikipedia.org/wiki/Raised-cosine$_{f}ilter, jan$2018.

[2] E. Axell, G. Leus, E. G. Larsson, and H. V. Poor. Spectrum sensing for cognitive radio : State-of-the-art and recent advances. *IEEE Signal Processing Magazine*, 29(3):101–116, May 2012. ISSN 1053-5888. doi: 10.1109/MSP.2012.2183771.

[3] G. Burel, C. Bouder, and O. Berder. Detection of direct sequence spread spectrum transmissions without prior knowledge. In *Global Telecommunications Conference, 2001. GLOBECOM '01. IEEE*, volume 1, pages 236–239 vol.1, 2001. doi: 10.1109/GLOCOM.2001.965114.

[4] O. A. Dobre, A. Abdi, Y. Bar-Ness, and W. Su. Survey of automatic modulation classification techniques: classical approaches and new trends. *IET Communications*, 1(2):137–156, April 2007. ISSN 1751-8628. doi: 10.1049/iet-com:20050176.

[5] A. Fehske, J. Gaeddert, and J. H. Reed. A new approach to signal classification using spectral correlation and neural networks. In *First IEEE International Symposium on New Frontiers in Dynamic Spectrum Access Networks, 2005. DySPAN 2005.*, pages 144–150, Nov 2005. doi: 10.1109/DYSPAN.2005.1542629.

[6] R. Harjani, D. Cabric, D. Markovic, B. M. Sadler, R. K. Palani, A. Saha, H. Shin, E. Rebeiz, S. Basir-Kazeruni, and F. L. Yuan. Wideband blind signal classification on a battery budget. *IEEE Communications Magazine*, 53(10):173–181, October 2015. ISSN 0163-6804. doi: 10.1109/MCOM.2015.7295481.

[7] A. Hazza, M. Shoaib, S. A. Alshebeili, and A. Fahad. An overview of feature-based methods for digital modulation classification. In *2013 1st International Conference on Communications, Signal Processing, and their Applications (ICCSPA)*, pages 1–6, Feb 2013. doi: 10.1109/ICCSPA.2013.6487244.

[8] J. Ma, G. Y. Li, and B. H. Juang. Signal processing in cognitive radio. *Proceedings of the IEEE*, 97(5):805–823, May 2009. ISSN 0018-9219. doi: 10.1109/JPROC.2009.2015707.

[9] S. Majhi and T. S. Ho. Blind symbol-rate estimation and test bed implementation of linearly modulated signals. *IEEE Transactions on Vehicular Technology*, 64(3):954–963, March 2015. ISSN 0018-9545. doi: 10.1109/TVT.2014.2327985.

[10] L. Mazet and P. Loubaton. Cyclic correlation based symbol rate estimation. In *Conference Record of the Thirty-Third Asilomar Conference on Signals, Systems, and Computers (Cat. No.CH37020)*, volume 2, pages 1008–1012 vol.2, Oct 1999. doi: 10.1109/ACSSC.1999.831861.

[11] Ingrid Moerman Merima Kulin, Tarik Kazaz and Eli de Poorter. End-to-end learning from spectrum data: A deep learning approach for wireless signal identification in spectrum monitoring applications. *Cornell University*, 2017.

[12] M. P. Olivieri, G. Barnett, A. Lackpour, A. Davis, and Phuong Ngo. A scalable dynamic spectrum allocation system with interference mitigation for teams of spectrally agile software defined radios. In *First IEEE International Symposium on New Frontiers in Dynamic Spectrum Access Networks, 2005. DySPAN 2005.*, pages 170–179, Nov 2005. doi: 10.1109/DYSPAN.2005.1542632.

[13] D. R. Pauluzzi and N. C. Beaulieu. A comparison of snr estimation techniques for the awgn channel. *IEEE Transactions on Communications*, 48(10):1681–1691, Oct 2000. ISSN 0090-6778. doi: 10.1109/26.871393.

[14] B. Ramkumar. Automatic modulation classification for cognitive radios using cyclic feature detection. *IEEE Circuits and Systems Magazine*, 9(2):27–45, Second 2009. ISSN 1531-636X. doi: 10.1109/MCAS.2008.931739.

[15] E. Rebeiz, F. L. Yuan, P. Urriza, D. Marković, and D. Cabric. Energy-efficient processor for blind signal classification in cognitive radio networks. *IEEE Transactions on Circuits and Systems I: Regular Papers*, 61(2):587–599, Feb 2014. ISSN 1549-8328. doi: 10.1109/TCSI.2013.2278392.

[16] Spooner. *Theory and Application of Higher-Order Cyclostationarity*. PhD thesis, UC Davis, Dept of Electrical and Computer Engineering,, 1992.

[17] A. Swami and B. M. Sadler. Hierarchical digital modulation classification using cumulants. *IEEE Transactions on Communications*, 48(3):416–429, Mar 2000. ISSN 0090-6778. doi: 10.1109/26.837045.

[18] B. Wang and K. J. R. Liu. Advances in cognitive radio networks: A survey. *IEEE Journal of Selected Topics in Signal Processing*, 5(1):5–23, Feb 2011. ISSN 1932-4553. doi: 10.1109/JSTSP.2010.2093210.

[19] Curtis M. Watson. *Signal Detection and Digital Modulation Classification-Based Spectrum Sensing for Cognitive Radio*. PhD thesis, Northeastern University, Boston, Massachusetts, The Department of Electrical and Computer Engineering, 2013.

[20] Dr.ir. Jos H. Weber. *Error-Correcting Codes*. Delft University of Technology, 2013.

[21] J. L. Xu, W. Su, and M. Zhou. Likelihood-ratio approaches to automatic modulation classification. *IEEE Transactions on Systems, Man, and Cybernetics, Part C (Applications and Reviews)*, 41(4):455–469, July 2011. ISSN 1094-6977. doi: 10.1109/TSMCC.2010.2076347.

[22] Zhechen Zhu and Asoke K. Nandi. *Automatic Modulation Classification Principles, Algorithms and Applications*. John Wiley & Sons, Ltd, 2015.